

2-14-2014

Material Characteristics of Hot Mix Asphalt and Binder Using Freeze-Thaw Conditioning

Ghazanfar Barlas

Follow this and additional works at: https://digitalrepository.unm.edu/ce_etds

Recommended Citation

Barlas, Ghazanfar. "Material Characteristics of Hot Mix Asphalt and Binder Using Freeze-Thaw Conditioning." (2014).
https://digitalrepository.unm.edu/ce_etds/88

This Thesis is brought to you for free and open access by the Engineering ETDs at UNM Digital Repository. It has been accepted for inclusion in Civil Engineering ETDs by an authorized administrator of UNM Digital Repository. For more information, please contact disc@unm.edu.

Ghazanfar Barlas

Candidate

Civil Engineering

Department

This thesis is approved, and it is acceptable in quality and form for publication:

Approved by the Thesis Committee:

Dr. Rafiqul A. Tarefder, Chairperson

Dr. Arup K. Maji

Dr. Mahmoud Reda Taha

**MATERIAL CHARACTERISTICS OF HOT MIX ASPHALT
AND BINDER
USING FREEZE-THAW CONDITIONING**

by

GHAZANFAR BARLAS

**B.S., CIVIL ENGINEERING
UNIVERSITY OF NEW MEXICO**

THESIS

Submitted in Partial Fulfillment of the
Requirements for the Degree of

**Master of Science
Civil Engineering**

The University of New Mexico
Albuquerque, New Mexico

December, 2013

DEDICATIONS

I would like to dedicate my work to my parents. My mother, who supported me in every step of life but unfortunately could not fight the battle of cancer. My father has been my motivation for pursuing a career in Civil Engineering.

ACKNOWLEDGMENTS

First and foremost, I would like to thank my parents, Shafiqah Ahmadi and Muhammad Nadir Ahmadi, who have supported me spiritually throughout my life and during my studies. Next, I would like to thank Professor Rafiqul A. Tarefder, my advisor, for his support and guidance during the time of my research. I would also like to thank Professor Arup K. Maji and Professor Mahmoud Reda Taha for their valuable time and being the members of my thesis committee. Also, I would like to thank the New Mexico Department of Transportation for their support: Jeff Mann (Head of Pavement Design, NMDOT), Parveez Anwar (State Asphalt Engineer, NMDOT), and Virgil Valdez (Research Bureau, NMDOT) for their valuable suggestions and continuous support. I owe my utmost gratitude to Hasan M. Faisal for his laboratory assistance, data analysis, and continuous support throughout my study. I would like to thank Md Rashadul Islam for his help and discussions. Lastly, I would like to thank my family, friends, and colleagues for their support during the completion of my thesis.

**MATERIAL CHARACTERISTICS OF HOT MIX ASPHALT
AND BINDER
USING FREEZE-THAW CONDITIONING**

by

Ghazanfar Barlas

B.S., Civil Engineering, University of New Mexico, 2011

M.S., Civil Engineering, University of New Mexico, 2013

ABSTRACT

Depending on the region, in a single year, the pavement undergoes many cycles of freezing and thawing. Freeze-thaw, as well as traffic loading, are important parameters in the study of damage in asphalt pavement. In areas of wide ranging temperatures, pavements are susceptible due to thermal cracking. This study investigates the effect of freeze-thaw on fatigue life and material characteristics of Hot Mix Asphalt (HMA) and binder. Since, temperature is variable throughout the year, a constant temperature should not be assumed when finding the fatigue life and material characteristics of HMA. To evaluate the damage, flexure test is conducted to determine the effect of freeze-thaw on the modulus and the fatigue life. In concurrence with the flexure test, indirect tensile (IDT) strength test is performed on the same mix with similar freeze-thaw conditioning to determine the reduction in the strength of HMA. Furthermore, Bending Beam Rheometer (BBR) test is performed on the binder that is used for the HMA. Similarly, the binder is

also subjected to freeze-thaw conditioning to determine the stiffness with respect to increasing freeze-thaw. The findings from this study show that freeze-thaw has a negative effect on HMA. The freeze-thaw conditioning decreases the stiffness by 5.3%, 5.9%, 9.0%, 16.8% and the fatigue life of the pavement by 35.8%, 36.1%, 53.6%, 37.4% for 5, 10, 15, and 20 freeze-thaw cycles, respectively. As the failure criteria for the four-point bending test is 50% of its initial stiffness, the reduction in initial stiffness due to freeze-thaw negatively affects the life of the pavement. The findings from the IDT strength test show a decrease in indirect tensile strength of AC by 0.8%, 2.0%, 2.2%, and 2.6% for 5, 10, 15, and 20 cycles of freeze-thaw. Although, a decrease in trend is seen, performing ANOVA analysis, the decrease in mean is statistically insignificant. The findings from the BBR test show that freeze-thaw causes damage to the binder, which can be seen in the reduction of stiffness with increasing freeze-thaw. The reduction in stiffness for 5, 10, 15, and 20 freeze-thaw cycles are 7.1%, 31.5%, 38.9%, and 41.1%, respectively.

Table of Contents

CHAPTER 1.....	1
INTRODUCTION.....	1
1.1. Problem Statement	1
1.1 Hypothesis	3
1.1.1 Hypothesis 1	3
1.1.2 Hypothesis 2	3
1.2 Outline	4
CHAPTER 2.....	5
LITERATURE REVIEW	5
2.1 Introduction	5
2.2 Current and Past Studies on Freeze-Thaw Conditioning Methods	5
2.3 Freeze-Thaw Conditioning Approaches	10
2.4 Four-Point Bending Test	11
2.5 Indirect Tensile Strength Test	12
2.6 Bending Beam Rheometer Test	13
2.7 Remarks	14
CHAPTER 3.....	15
SAMPLE PREPARATION AND LABORATORY TESTING	15
3.1 Experimental Plan	15
3.2 HMA Mixture Gradation	15
3.3 Sample Preparation	17
3.3.1 Beam Specimen	17
3.3.2 Cylindrical Specimen	19
3.3.3 BBR Specimen	21
3.4 Sample Cutting	23
3.4.1 Asphalt Beam Samples	23
3.4.2 Asphalt Cylinder Samples	25
3.5 Specimen Volumetric Analysis	26
3.6 Sample Conditioning	27
3.7 Four-Point Bending Test	29
3.8 Indirect Tensile Strength Test	32
3.9 Bending Beam Rheometer Test	35
CHAPTER 4.....	38
EFFECT OF FREEZE-THAW ON BEAM FATIGUE PARAMETERS	38
4.1 Introduction	38
4.2 Fatigue Test	39
4.2.1 Results and Discussion on Beam Fatigue Test	39
CHAPTER 5.....	54

EFFECTS OF FREEZE-THAW ON INDIRECT TENSILE STRENGTH AND BENDING BEAM RHEOMETER STIFFNESS	54
5.1 Introduction	54
5.2 Indirect Tensile Strength Test	56
5.2.1 Results and Discussion for IDT Test.....	56
5.3 Bending Beam Rheometer Test	62
5.3.1 Results and Discussion for BBR Test.....	62
CHAPTER 6.....	71
CONCLUSIONS AND RECOMMENDATIONS	71
6.1 Conclusions	71
6.1.1 Fatigue Test Conclusion	71
6.1.2 IDT Test Conclusion	72
6.1.3 BBR Test Conclusion	73
6.2 Recommendations for Future Work	73
REFERENCES	74

LIST OF FIGURES

Figure 3.1: Aggregate Gradation for SP-III Mixture	16
Figure 3.2: Linear Kneading Compactor	18
Figure 3.3: Linear Kneading Compactor Mold	18
Figure 3.4: Pine Gyrotory Compactor	20
Figure 3.5: Molded Sample with 8 inches Height and 6 inches Diameter	20
Figure 3.6: Trimming of Room Temperature Binder Sample	21
Figure 3.7: Finished BBR sample	22
Figure 3.8: Finished sample conditioning of Binder Sample in -10°C.....	22
Figure 3.9: Uncut Hot Mix Asphalt Beam Samples	23
Figure 3.10: GCTS stone-cutting saw with original clamps.....	24
Figure 3.11: GCTS stone-cutting saw with modified clamps.....	24
Figure 3.12: GCTS Pressure Controlled Core Drill.....	25
Figure 3.13: Espec Temperature/Humidity Chamber.....	28
Figure 3.14: Samples Being Conditioned by Freeze-Thaw Method.....	28
Figure 3.15: Typical Four-Point Bending Test Schematic	29
Figure 3.16: GCTS Flexural Beam Setup.....	31
Figure 3.17: Beam Fatigue Test Setup with the LVDT Attached.....	31
Figure 3.18: IDT Sample with Dimensions	33
Figure 3.19: IDT Asphalt Concrete Sample	33
Figure 3.20: IDT Test Setup with a Specimen	34
Figure 3.21: BBR Sample with Dimensions	36
Figure 3.22: BBR Testing Apparatus	36
Figure 3.23: BBR Test Setup with a Sample.....	37
Figure 4.1: Stiffness versus Different Numbers of Freeze-Thaw Cycles Curve	40
Figure 4.2: Comparison of Number of Cycles to Failure with Different Freeze-Thaw Cycles	41
Figure 4.3: Comparison of Stiffness Reduction with Different Freeze-Thaw Cycles	42
Figure 4.4: Stiffness versus Number of Cycles for 0 Freeze-Thaw Cycles.....	44
Figure 4.5: Stiffness versus Number of Cycles for 5 Freeze-Thaw Cycles.....	44
Figure 4.6: Stiffness versus Number of Cycles for 10 Freeze-Thaw Cycles.....	45
Figure 4.7: Stiffness versus Number of Cycles for 15 Freeze-Thaw Cycles.....	45
Figure 4.8: Stiffness versus Number of Cycles for 20 Freeze-Thaw Cycles.....	46
Figure 4.9: Stiffness Ratio versus Number of Cycles for 0 Freeze-Thaw Cycles	47
Figure 4.10: Stiffness Ratio versus Number of Cycles for 5 Freeze-Thaw Cycles	47
Figure 4.11: Stiffness Ratio versus Number of Cycles for 10 Freeze-Thaw Cycles	48
Figure 4.12: Stiffness Ratio versus Number of Cycles for 15 Freeze-Thaw Cycles	48

Figure 4.13: Stiffness Ratio versus Number of Cycles for 20 Freeze-Thaw Cycles	49
Figure 4.14: Correlation of Initial Stiffness with Increasing Number of F-T Cycles	50
Figure 4.15: Box Plot for Different Cycles of F-T with Their Respective Initial Stiffness.....	51
Figure 4.16: Correlation of Number of Cycles to Failure to F-T Cycles.....	52
Figure 4.17: Box Plot for No. of Cycles to Failure with Respective F-T Cycles	53
Figure 5.1: Comparison of IDT Strength with different Freeze-Thaw Cycles	59
Figure 5.2: Strength Reduction with Different Freeze-Thaw Cycles	59
Figure 5.3: Comparison of Tensile Strength Ratio with different Freeze-Thaw Cycles	60
Figure 5.4: Box Plot for IDT Strength with Respective F-T Cycles	61
Figure 5.5: Test Data Plot Obtained for Asphalt Binder for 20 cycles of F-T.....	63
Figure 5.6: Displacement over Time for 0 F-T Cycles.....	64
Figure 5.7: Displacement over Time for 5 F-T Cycles.....	64
Figure 5.8: Displacement over Time for 10 F-T Cycles.....	65
Figure 5.9: Displacement over Time for 15 F-T Cycles.....	65
Figure 5.10: Displacement over Time for 20 F-T Cycles.....	66
Figure 5.11: Stiffness with Respect to Freeze-Thaw Cycles	66
Figure 5.12: plot of stiffness vs. logarithmic time for m-value calculation for 60 sec.	68
Figure 5.13: Box Plot for different cycles of F-T with their respective Stiffness.....	68
Figure 5.14: m-value Box Plot for Each Class of Freeze-Thaw Cycle.....	69

LIST OF TABLES

Table 3.1: Aggregate Gradation for SP-III.....	16
Table 4.1: Fatigue Test Results with Different Cycles of Freeze-Thaw.....	42
Table 5.1: Test Matrix for IDT Test.....	55
Table 5.2: Test Matrix for Bending Beam Rheometer Test	55
Table 5.3: Laboratory Indirect Tensile Strength and Tensile Strength Ratio	57
Table 5.4: Stiffness and m-value Test Results for BBR	70

CHAPTER 1

INTRODUCTION

1.1. Problem Statement

Hot Mix Asphalt (HMA) in pavement structures has been used throughout United States and worldwide. As more research is being done, there have been significant changes in the way pavements are built today. Design standards are constantly updated and changing with new ways of analyzing and predicting the behavior of HMA. Pavements are built with several criteria in mind and depending on the location of the pavement, different mix designs, traffic intensity, and climatic factors are taken into consideration.

The design of asphalt pavements mainly focuses on resisting rutting, low temperature cracking, and fatigue cracking. With the use of Performance Grade (PG) binders, the rutting issue can be addressed on the binder level. Climate plays a major role in traffic induced fatigue and low-temperature cracking. Pavement experiences various weather conditions as well as high intensity traffic loading over a certain period of time. Consequently, the latest testing in time dependent testing of asphalt is needed, along with a similar weathering condition. One of the common weather patterns a pavement experiences is freezing and thawing. Kestler et al, (2011) found that there is a correlation between the fatigue damage (Asphalt Institute) and winter season weather pattern. Statistical study indicated that more fatigue damage occurs in shorter winters as well as warmer winters with shallow freeze-thaw depths. To address this issue, the use of freeze-thaw conditioning is recommended to represent the field conditions.

Freeze-thaw damage, as well as traffic loading, are important parameters in life of asphalt pavement. As the weather is not constant throughout the year, it gets cold in the winter and hot in the summer, it is not feasible to assume a constant temperature when trying to find the fatigue life and material characteristics of HMA. Depending on the region, in a single year, the pavement undergoes many cycles of freezing and thawing (Goh and You 2012; Attia and Abdelrahman 2010; Loria et al, 2011; Bolzan 1989; Ozgan and Serin 2012; Feng et al, 2010; Chen and Huang 2007; Lu and Harvey 2008). Some researchers have shown, through indirect tensile test, that after each cycle of freezing and thawing, the tensile strength ratio decreases (Chen and Huang 2007; Feng et al, 2010; Shu et al, 2012; Loria et al, 2011).

In 2010, Mei et al, researched the fatigue life of asphalt pavement and in the study, splitting fatigue test was performed. The two major drawbacks of this study was there was no comparison between several freeze-thaw cycles and of lately, most researchers use four-point bending tests to determine the fatigue life of asphalt pavements because of its ability to better predict fatigue life. A study needs to be conducted on the effects of freeze-thaw cycles on asphalt pavement through the use four-point bending test to understand its effect on pavement life. Another objective of this thesis is to relate the asphalt binder's creep stiffness as a function of time and also perform indirect tensile strength of asphalt concrete when it has been subjected to freeze-thaw cycles.

1.1 Hypothesis

1.1.1 Hypothesis 1

Although in the previous research, it is shown that freeze-thaw has a negative effect on the engineering properties of asphalt, strength of asphalt samples have shown to decrease. Little to no work has been done to find the effect of freeze-thaw on the fatigue life and stiffness of asphalt material. It hypothesized that the same negative effect may occur on the fatigue life and stiffness of asphalt as well. This hypothesis can be proven by inducing freeze-thaw conditioning and performing four-point bending test on asphalt samples and Bending Beam Rheometer test on the binder.

1.1.2 Hypothesis 2

In previous research, done on the strength of asphalt, it has been shown that most damage occurs during the first stages of freeze-thaw and then decreases steadily with every cycle of freeze-thaw. It can be hypothesized that same damage trend may occur for local NM mixes. The fatigue life will be affected the most with the first freeze-thaw conditioning and decrease slowly. An equation can be developed which can relate damage of asphalt with the number of freeze-thaw cycles. Moreover, from the initial stiffness of asphalt, a prediction can be made to determine the stiffness of the pavement after a given number of freeze-thaw cycles. Furthermore, the results from IDT tests may support the findings of the fatigue tests. A model can be created to describe the damage occurring after freeze-thaw for the IDT test.

1.2 Outline

In this study, the effect of freeze-thaw conditioning on the HMA and binder is introduced. Freeze-thaw conditioning is used in conjunction with four-point bending test, indirect tensile strength test, and bending beam rheometer test.

This thesis will include 6 chapters: Introduction, literature review, sample preparation and laboratory testing, effect of freeze-thaw on beam fatigue parameters, effect of freeze-thaw on indirect tensile strength and bending beam rheometer stiffness, and Conclusion.

Chapter Two, the literature review, summarizes moisture damage (freeze-thaw) to asphalt and their relations to the present study.

Chapter Three, sample preparation and laboratory testing, describes the experimental plan for this study. This chapter includes material selection, sample preparation, sample conditioning, laboratory fatigue testing, indirect tensile strength testing and bending beam rheometer testing.

Chapter Four, effect of freeze-thaw on beam fatigue parameters, will include the laboratory data and analysis which has been obtained from the freeze-thaw conditioning.

Chapter Five, effect of freeze-thaw on indirect tensile test and bending beam rheometer test, will include the laboratory data and analysis which has been obtained from the freeze-thaw conditioning.

Chapter Six is the concluding chapter for this study. This chapter summarizes the findings from the laboratory tests with freeze-thaw conditioning.

CHAPTER 2

LITERATURE REVIEW

2.1 Introduction

This chapter presents a summary of moisture induced freeze-thaw conditioning of asphalt material and its relevant testing methods by previously conducted and on-going research.

2.2 Current and Past Studies on Freeze-Thaw Conditioning Methods

Moisture Damage is one of the major concerns in asphalt pavements. Moisture damage can be described in two different stages, loss of adhesion and loss of cohesion. Loss of adhesion, which is the stripping of asphalt film, occurs between the asphalt and the aggregate. This phenomenon is called “stripping”. Loss of cohesion happens within the binder itself due to water infiltration and causes a loss of mixture stiffness, which a complex phenomenon affected by many factors.

Moisture related damage can be attributed by a lot of distresses in pavement. Some of the factors the can contribute to moisture related distress are the mix design (binder type, binder content, aggregate, air voids, and additives), production of the Hot Mix Asphalt (HMA), Construction (compaction, permeability, reproducibility), and most importantly Climate (freeze-thaw, rainfall, excessive heat). Some other factors which affect the life and durability of asphalt pavements are surface drainage, subsurface drainage, rehab strategies and truck volume).

Asphalt is a viscoelastic material, which means it can heal if given enough time. Cracks in the pavement occur due to many climatic, traffic, and construction reasons. The major reason as to why pavement collapse fail at a faster rate is the repeated truck traffic and

freeze-thaw cycles (Garcia, 2011). Garcia found that the healing rates of asphalt mastic increases with the increase of temperature. Although, it is possible for the asphalt mastic to heal, it is complex to predict the healing time and temperature which is a function of the aging and the binder type.

There are limited researches dedicated to the study of freeze-thaw on asphalt pavement. Work by Feng et al., 2009 showed that freeze-thaw damage occurs in three different stages. Feng concluded that with the increase of freeze-thaw cycles, the splitting strength of asphalt decreased, weight loss rate decreased while the volume of the mix expanded in a steady manner. Feng also noted that the performance stabilized until the next rapid deterioration caused by loss of adhesion. Indirect tensile strength tests were performed at 0, 2, 4, 6, 8 cycles of freeze-thaw conditioning. However, to understand the behavior of the pavement, a fatigue test is required to capture the deterioration over a number of years.

Mei et al., 2010 at Jiaotong University in China reported that fatigue life of asphalt pavements in rich rainfall areas are about 60% of that in a drought or little rain area. It was also noticed that the better fatigue life was observed as the pavement thickness increased. This of course will lead to a higher pavement cost which is not plausible. Mei adopted the test method of split fatigue test which uses a stress controlled method to define the fatigue life. Stress controlled method is acceptable when the thickness of the pavement is greater than 5 inches (125 mm). With the use of different pavement design methods, more pavement are designed with different layers and most asphalt layer close to the top surface have a thickness of less than 5 inches. Since the most damage occurs

towards the top, constant strain test would yield a more accurate representation of the pavement life.

In another study by Feng et al., 2010, which relates the impact of salt versus distilled water with the conditioning method of freeze-thaw, it was found that freeze-thaw damage of asphalt mixtures include two phases. In first phase, the damage is caused by the expansion of water which would ultimately decrease the indirect tensile strength of the asphalt. The damage of the second phase occurs on the interfacial of the mix between the asphalt and the aggregate or in some cases, the fracture of asphalt mortar which results in weight loss. It was also found that salt plays a major role in the low temperature performance of asphalt binder. Particularly, when the percentage of salt is greater than 3, the deformability of asphalt decreases rapidly. However, no attempt was done in this study to relate the fatigue life of the pavement.

While in an attempt to figure out the effect of freeze-thaw on the fatigue life of asphalt, other researcher have investigated certain engineering characteristics of asphalt being exposed to freeze-thaw conditioning. Ozgan and Serin (2012) investigated effect of freeze-thaw on the binder and wearing surface coats. In this particular study, specimens were exposed to freeze-thaw cycles for 6, 12, 18, and 24 days after which the voids ratios fill with asphalt, void ratio, and the voids ratios inside the aggregate were determined by the method of ultrasonic velocity and Marshall Stability. Ultrasonic Velocity is a test done on materials to measure their acoustic velocity in order to measure some mechanical properties. The findings from the research concluded that there are important negative effects of the freeze-thaw on the engineering properties of asphalt mixture.

Another form of moisture inducing method which has been used recently is Moisture Sensitivity Stress Tester (MIST). MIST is used for testing the moisture susceptibility of asphalt mixtures which is designed to simulate the stripping mechanisms that occur in the HMA pavement. Shu et al., (2012) used MIST as well as freeze-thaw conditioning of plant-produced foam warm mix asphalt with a high percentage of Reclaimed Asphalt Pavement (RAP) to evaluate the moisture susceptibility of the mix. In the study, indirect tensile test (IDT), tensile strength ratio (TSR), dynamic modulus test, and Asphalt Pavement Analyzer (APA) Hamburg tracking test were used to evaluate the effect of MIST and freeze-thaw conditioning. It was concluded that both freeze-thaw and MIST had different effects on the properties of asphalt. IDT induced greater damage to IDT strength, which is often used to determine the fatigue life, while MIST had greater impact on the Dynamic Modulus. It can be reasonable to conclude that freeze-thaw method induces greater damage to asphalt pavement and can be used as a superior to MIST to induce maximum damage to asphalt pavement for determining fatigue life. Loria et al., (2011) also concluded that the use of multiple freeze-thaw cycles provide a better characterization of the mixture's reaction to moisture damage.

Another method to evaluate the effects of moisture and freeze-thaw cycles can be analyzed with Freeze-Thaw Pedestal Test (FTPT) developed by Plancer et al (1980). FTPT is a water susceptibility test that indicates the susceptibility of asphalt-aggregate mixtures to repeated freeze-thaw cycles (Bolzan 1989).

Attia and Abdelrahman (2010) studied the effect of freeze-thaw conditioning, RAP content, moisture content, as well as dry density to access the structural capacity of RAP. Attia and Abdelrahman evaluated the effect of freeze-thaw on RAP and concluded that

the Resilient Modulus, when compacted at 2% above optimum moisture content, increased after freeze-thaw conditioning yet did not show loss of strength when compacted at optimum moisture content. Not having a negative impact of the stiffness of RAP can be explained by the low ability of RAP to hold extra moisture beyond optimum. To find the future stiffness of the RAP, a fatigue test is ideal to represent the stiffness reduction after certain amount of time.

More freeze-thaw occurs when the temperature are not very extreme and close to freezing point. This allows the temperature to fluctuate more often below and above freezing. In return, the pavement experiences more freeze-thaw cycles which causes the pavement more distress. In a statistical study done by Kestler et al, (2011), it was noted that moderate correlation between the fatigue damage (Asphalt Institute) and winter season characteristics indicated that more fatigue damage occurs in shorter winters as well as warmer winters with shallow freeze-thaw depths. The past studies, similar patterns have been observed where short and warm winters imply temperatures closer to freezing, resulting in more freeze-thaw cycles. To understand the damage of each freeze-thaw cycles, laboratory tests have to be done to see the effect for every cycle of freezing and thawing.

Damage mostly occurs on the surface of the asphalt pavement where it experiences the most amount of temperature deviation. In hot weather, the top surface experiences the most heat which results in aging and oxidation of the binder. In cold weather, the top surface experiences the most cold and the moisture from the air is induced in the pavement. Goh and You (2012) studied the stripping of fine and coarse aggregates on the surface of the asphalt mixture after being freeze-thaw conditioned. The effect of freezing

and thawing was then analyzed using an image processing technique. Samples were conditioned for a total of 38 days with 8 freeze-thaw cycles per day. It was concluded that distresses of cracks and stripping increase with each freeze-thaw cycles. To further confirm this study, work has to be done on the performance of the asphalt mixture after being induced to freezing and thawing.

2.3 Freeze-Thaw Conditioning Approaches

The climate is a big factor in determining the procedures of freeze-thaw methods. Many different methods have been explored by many researchers to find the freezing and thawing temperatures, freeze-thaw durations, and number of cycles appropriate. Attia and Abdelrahman (2010) uses the freeze-thaw conditioning method of freezing the specimen for 24 hours at -24°C followed by 24 hours of thawing at 24°C. Samples were subjected to two freeze-thaw cycles. By subjecting the samples to long term freezing and thawing, it becomes difficult to observe what actually happens in between and how the sample is being damaged. To better understand the damage of freeze-thaw, shorter freezing and thawing should be incorporated.

Goh and You (2012) subjected the samples into an automatic freeze-thaw chamber for 38 days. Each day samples were subjected to 8 freeze-thaw cycles for a total of 300 cycles. A single freeze-thaw cycle consisted of freezing the sample to 0°F (-17.8°C) and steadily raising the temperature to 40°F (4.4°C). This method of freeze-thaw creates great amount of damage due to the amount of freeze-thaw cycles. Ozgan and Serin (2012) uses a total of 24 cycles of freeze-thaw, while Feng et al, (2010) uses 8 cycles to condition the samples. Feng et al, (2010) conditioned the samples with water conditioning by vacuum saturation with distilled water for 15 minutes. Then the specimen were subjected to

freezing for 8 hours at -20°C followed by soaking for 4 hours at 60°C , a total of 2 cycles per day. Chen and Huang (2007) subjected the samples to one and two freeze-thaw cycles with the conditioning method in accordance to ASTM D4867. Shu et al, (2012) conducted only one freeze-thaw cycles on the specimen. It can be seen, many different conditioning method have been explored by different researchers. One important factor which was not addressed by the previous study is thermal shock. The previous studies show thermal shock is neglected, which does not represent the field condition. In the field, the temperature gradually changes; it takes time for temperature in the field to go from its maximum negative to maximum positive. In this research, the issue of neglecting thermal shock will be addressed.

One of the freeze-thaw conditioning in concrete is the ASTM C1645. This procedure gives the standard for rapid freezing and thawing of concrete. Although, this standard is for concrete, same procedure can be used to condition asphalt pavement. This standard consists of freezing at -5°C (27°F) for 16 hours and thawing at 30°C (86°F) for 8 hours. This method is the most reasonable conditioning method because on average during winters, in North America and Canada, the air temperature is below freezing for the majority of the 24 hour duration and above freezing the least amount of time.

2.4 Four-Point Bending Test

There have been many studies done to evaluate the most appropriate method for defining the fatigue behavior of asphalt concrete material. Coni et al. (2008) reported that in a recent interlaboratory campaign, 11 different test methods were evaluated which included uniaxial tension/compression, 2-point bending test, 3-point bending test, 4-point bending test, indirect tension tests. It was concluded that fatigue behavior affected by test method.

In another study by Tangella et al. (1990), it was concluded that the repeated flexure test received the highest approval and gave the most representative fatigue behavior amongst other test methods. From the previously done research and current practice, the most effective test method is four-point bending test.

The four-point bending test is the most common test used to determine the fatigue behavior of asphalt concrete. Four-point bending test subjects the middle one-third of the beam to pure bending, hence, no shear deformation. The standard used for the beam fatigue is AASHTO T 321 and ASTM D7460. Typically, two loading modes are used: controlled strain and controlled stress. Controlled strain is used for thinner pavement, whereas, controlled stress is used for pavement with thicker sections. The number of cycles at 50% of its initial stiffness can be considered the fatigue life of the asphalt mixture for that particular tested strain or stress level. Although, previously some researchers (Pell and Cooper, 1975; Tayebali et al., 1992; Rowe, 1993) have used constant stress, the common practice is to test with a constant strain mode, which is also the standard in AASHTO T 321.

2.5 Indirect Tensile Strength Test

Indirect tensile (IDT) strength test is an important test in designing a pavement structure. With the recent use of Mechanical Empirical Pavement Design Guide (MEPDG) developed by AASHTO, the tensile strength plays an important parameter in predicting the low temperature cracking in asphalt pavement.

In 1978, Lottman presented in a NCHRP report the procedure of testing asphalt cylindrical sample. He proposed the Lottman procedure, in which the specimens are 4 inches in diameter and 2.5 inches in height and the air void content target to be between 4

to 8%. The procedure was then finalized as AASHTO T 322 to test indirect tensile strength of samples.

Another standard, AASHTO T 283, which determines the resistance of compacted bituminous mixture to moisture damage, is also widely used. This method is used to determine the change diametral tensile strength from conditioning in the laboratory. This method is the most appropriate method in testing cylindrical asphalt samples and finding the tensile strength.

2.6 Bending Beam Rheometer Test

In areas of wide ranging temperatures, asphalt pavements are susceptible due to thermal cracking. Thermal cracking is related to the stiffness of asphalt binder at low temperature. BBR is a simple test to measure the flexible creep stiffness of the asphalt binder at low temperature range of $-40\text{ }^{\circ}\text{C}$ to $0\text{ }^{\circ}\text{C}$ in accordance with AASHTO T 313. An asphalt beam used for this test has dimensions of $125\times 6.25\times 12.5$ mm. The point load of 980 mN is applied on the asphalt beam for 240 seconds. By measuring beam deflection, stiffness is calculated. Stiffness value is related to the thermal stresses of asphalt, whereas m-value refers to the stress relaxation ability of the material.

2.7 Remarks

This chapter has discussed the previous and ongoing research on the freeze-thaw conditioning of asphalt material. Although, there have been some research done to find some engineering properties of asphalt after freeze-thaw, no attempt has been done to study the fatigue life of asphalt pavement over several freeze-thaw cycles using the four-point bending test. In chapter 3, the research method will be discussed on fatigue life of asphalt as well as other characteristic tests such as IDT strength test and BBR test.

CHAPTER 3

SAMPLE PREPARATION AND LABORATORY TESTING

3.1 Experimental Plan

SP-III, commonly used in New Mexico Highways, with PG 70-22 binder is used for this study. SP-III is mostly used due to its resistance to fatigue cracking and is used in the intermediate layer of pavement structure.

Hot Mix Asphalt mixture is collected from the construction site for testing purposes. Samples are collected in accordance with AASHTO T-168 for bituminous mixtures. Bags of 15kg samples are collected directly from the road site. 15kg is the most efficient weight for sampling and later for heating the sample for compaction. On average a single slab for preparing beam samples is 12kg, 3kg extra is taken for material loss while heating and transporting.

3.2 HMA Mixture Gradation

Table 3.1 shows aggregate gradations of SP-III mixture samples. Upper and lower limits of the mix are also shown in table 3.1. It can be seen that the sample gradation falls within the NMDOT specification for SP-III mix. Figure 3.1 represents the aggregate gradation chart for SP-III mixture. The maximum density line for maximum aggregate sizes of 1 inch is plotted. The mixture plots below the maximum density line, which represents a coarser mix.

Table 3.1: Aggregate Gradation for SP-III

Sieve Size	NMDOT SP-III Specification		Percent Passing
	Lower Limit (%)	Upper Limit (%)	
1"	100	100	100.0
3/4"	90	100	96.0
1/2"	-	90	71.0
3/8"	50	66	58.0
#4	31	45	38.0
#8	23	49	24.0
#16	-	-	15.0
#30	-	-	11.0
#50	-	-	8.1
#100	-	-	6.0
#200	2	8	4.4

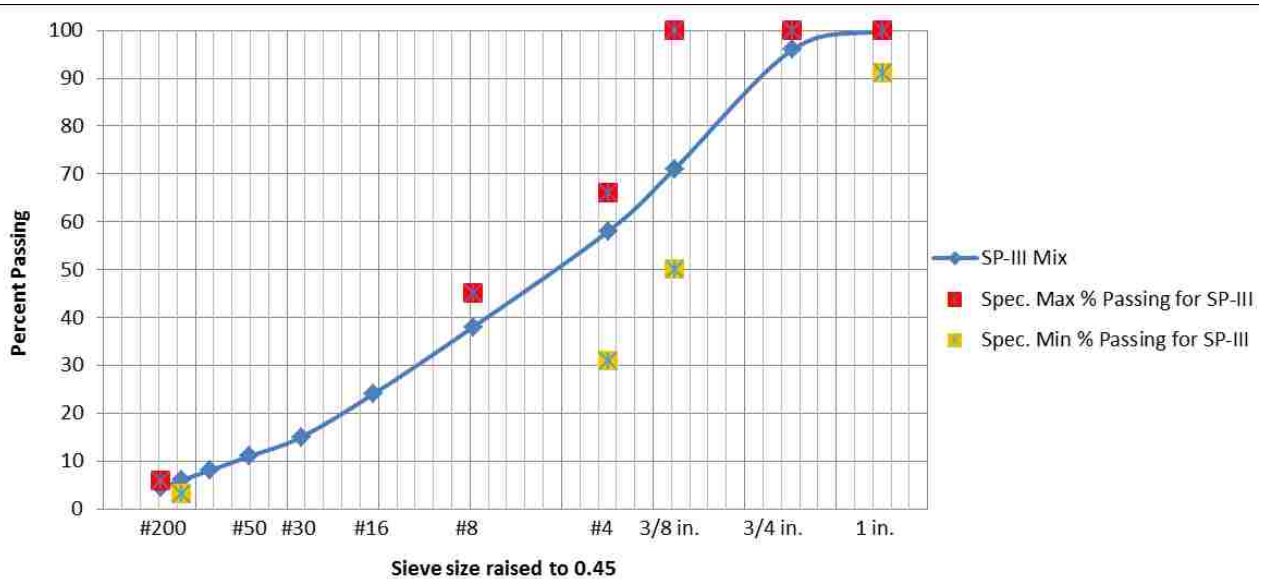


Figure 3.1: Aggregate Gradation for SP-III Mixture

3.3 Sample Preparation

3.3.1 Beam Specimen

According to AASHTO T321, a sample size of 380 mm x 65 mm x 50 mm (15" x 2.5" x 2") must be achieved for the testing of laboratory beam fatigue testing. Samples are heated and transferred in accordance with AASHTO T312. A target heating temperature 280°F and a target molding temperature of 280°F is achieved (NMDOT Specifications). The samples are heated for no more than an hour and a half to ensure no additional aging occurs. The weights of samples are taken using a digital scale to ensure accuracy and are then transferred to the compactor.

Linear kneading compactor shown in figures 3.2 and 3.3, is constructed of stainless steel and 1045 steel and powered by 208/230 Volt 3-Phase, to create beam slabs. The compactor is operated by a hydraulic unit. The compactor has the capability of creating a larger than the standard samples, at which point, the slab is cut from all directions to achieve a final smooth beam of 380 mm x 65 mm x 50 mm (15" x 2.5" x 2").



Figure 3.2: Linear Kneading Compactor



Figure 3.3: Linear Kneading Compactor Mold

3.3.2 Cylindrical Specimen

Cylindrical sample are prepared using a pneumatic gyratory compactor. The compactor is equipped to set the maximum number of gyrations of the mold or a minimum height requirement for the sample inside the mold. The gyratory compactor produces sample sizes of 8 inches high and 6 inches in diameter. As with the beam samples, the target heating temperature 280°F and a target molding temperature of 280°F is achieved (NMDOT Specifications). The samples are heated for no more than an hour and a half, until workable. The weights of samples are taken using a digital scale and are then transferred to the compactor. Figure 3.4 shows the gyratory compactor and figure 3.5 shows a molded sample with a height of 8 inches and diameter of 6 inches.



Figure 3.4: Pine Gyrotory Compactor



Figure 3.5: Molded Sample with 8 inches Height and 6 inches Diameter

3.3.3 BBR Specimen

BBR samples are prepared in accordance to AASHTO T 313. Samples sizes are 6.25 mm x 12.5mm x 100mm. The binder is heated at 300°C and heated long enough until it is in workable fluid state. During the heating process, samples must be covered and also stirred to ensure equal aging and homogeneity. This procedure will remove air bubbles to avoid any voids in the specimen. In a mold, the binder is poured. The sample is trimmed, seen in figure 3.6, and taken out of the mold after 45 to 60 minutes of cooling. The finished sample, at room temperature, can be seen in figure 3.7. The binder beam samples must be in a bath at the desired testing temperature for 60 minutes for conditioning, seen in figure 3.8.



Figure 3.6: Trimming of Room Temperature Binder Sample



Figure 3.7: Finished BBR sample

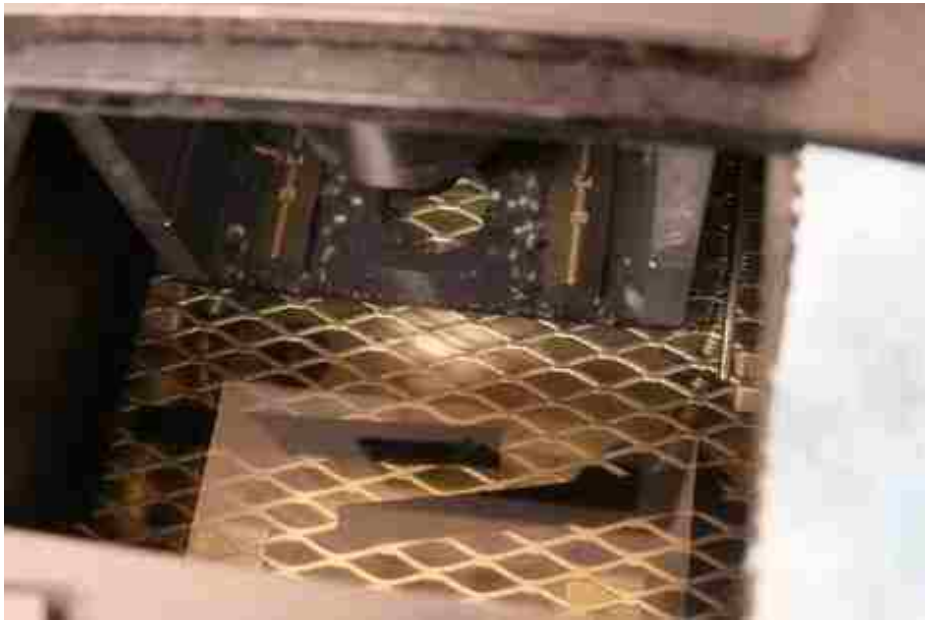


Figure 3.8: Finished sample conditioning of Binder Sample in -10°C

3.4 Sample Cutting

3.4.1 Asphalt Beam Samples

The linear kneading compactor produces samples sizes of 18" x 6" x 3", show in figure 3.9. Samples must be cut to 15" x 2.5" x 2". Using GCTS stone-cutting saw shown in figures 3.10, each slab is cut and trimmed of all sides to achieve a smooth outer surface. Originally, the GCTS saw was not intended to cut beam samples, an entire new clamping system was designed which is capable of clamping a beam sample of such size. The new clamp, which is shown in figure 3.11, allows for better precision cutting of long samples. Previously, the GCTS saw was only capable of cutting short samples.



Figure 3.9: Uncut Hot Mix Asphalt Beam Samples



Figure 3.10: GCTS stone-cutting saw with original clamps



Figure 3.11: GCTS stone-cutting saw with modified clamps

3.4.2 Asphalt Cylinder Samples

The gyratory compactor produces sample sizes of 8 inches high and 6 inches in diameter. The standard for IDT, AASHTO T 283, calls for samples sizes to be 4 inches (100mm) in diameter and 2.5 ± 1 inches (63.5 ± 2.5 mm) in thickness. The compacted sample must first be cored to a 4 in diameter thickness using GCTS Pressure Controlled Core Drill seen in figure 3.12. Once, the correct diameter is achieved, the sample is then cut using GCTS stone-cutting saw.



Figure 3.12: GCTS Pressure Controlled Core Drill

3.5 Specimen Volumetric Analysis

Maximum Specific Gravity (G_{mm}) is done in accordance with ASTM D6857. The CoreLok system, which is a system for sealing asphalt samples so that the sample densities are measured, is used as an alternative to the conventional “Rice Test” for the determination of maximum specific gravity of loose asphalt mixtures. The Corelok automatically seals the samples in a puncture resistant polymer bags. The samples are dried previously and then placed inside the vacuum bags. The bags are sealed with the CoreLok vacuum chamber. Then, the bags are cut open under water and the weight is taken while the sample is still submerged in water. Average G_{mm} for the mix used is 2.516. The calculations for determining G_{mm} are as follows:

$$G_{mm} = \frac{A}{A-(C-B)} \quad (3.1)$$

Where,

A = weight of dry sample in air, (grams)

B = weight of bag, (grams)

C = weight of sample open in water, (grams)

Bulk specific gravity (G_{mb}) is performed on asphalt beam samples according to AASHTO T269. The weight of the sample is taken under three different conditions: dry, saturated surface dry, and submerged in water. G_{mb} can be calculated using the following:

$$G_{mb} = \frac{A}{B-C} \quad (3.2)$$

Where,

G_{mb} = Bulk specific gravity

A = Mass of sample in Air

B = Mass of sample saturated surface dry

C = Mass of sample submerged in water

The target air voids in the compacted mixture for this study is between 5 and 6%. The air voids can be calculated using following:

$$VTM = 1 - \frac{Gmb}{Gmm} \quad (3.3)$$

Where,

VTM = Air voids in the compacted mixture

3.6 Sample Conditioning

Samples are conditioned according to ASTM C1645 which calls for freezing at -5°C for 16 hours and $+30^{\circ}\text{C}$ for 8 hours. -5°C and $+30^{\circ}\text{C}$ are chosen as target temperatures because they represent field conditions. In New Mexico, air temperatures reach on average of -5°C during winter and $+30^{\circ}\text{C}$ is a representative temperature to thaw the HMA. Moreover, by having greater freezing time, it simulates more damage in the HMA due to ice forming in the HMA and expanding. After completing these two stages, it is considered one cycle. As well as conditioning the samples to freezing and thawing, humidity is also included. At -5°C , at humidity level of 15% is induced, which is the average humidity in December in New Mexico. At $+30^{\circ}\text{C}$, a humidity level of 40% is induced. The freeze-thaw and humidity conditioning is done with an Espec temperature/humidity chamber, shown in figure 3.13 and 3.14. The Espec chamber is an automatic temperature/humidity controller. This reduces the risk of any human error.



Figure 3.13: Espec Temperature/Humidity Chamber



Figure 3.14: Samples Being Conditioned by Freeze-Thaw Method

3.7 Four-Point Bending Test

There are several different tests for determining the fatigue life of Hot Mix Asphalt (HMA) but recent research indicates the Four-point bending is the most effective and commonly used HMA fatigue test. The standard for this bending beam fatigue test is AASHTO T321. The Four-point flexural test subjects an asphalt beam sample to a repeated bending with a controlled strain level, frequency, and chamber temperature. The figure of a typical four-point bending test can be seen in figure 3.15.

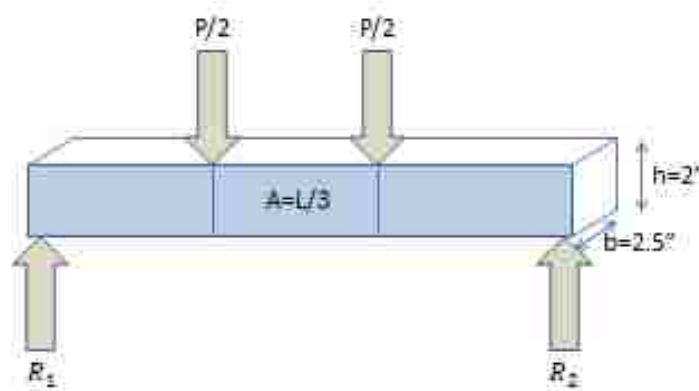


Figure 3.15: Typical Four-Point Bending Test Schematic

The test is performed using GCTS Flexural Beam setup shown in figure 3.16. Using the deflection history, load response history, and geometry of test specimen, the maximum strain and stress in specimen is calculated using equations 3.4 and 3.5, respectively. The data is collected using CATS software which is also used to control the test.

$$\varepsilon = \frac{12 h \delta}{3L^2 - 4a^2} \quad (3.4)$$

$$\sigma = \frac{P L}{b h^2} \quad (3.5)$$

Where,

ε = maximum strain

σ = maximum stress

P = load applied by actuator at time t

b = average specimen width

h = average specimen height

δ = deflection at center of beam at time t

a = distance between inside clamps

L = distance between outside clamps.

Sample flexural stiffness is then calculated using σ and ε data recorded from each cycle.

$$E = \frac{\sigma_t}{\varepsilon_t} \quad (3.6)$$

Where,

E = flexural modulus

Then, number of cycles at 50% reduction in stiffness is recorded as failure of beam according to AASHTO T 321. Testing is conducted in constant strain mode. Each beam sample is sinusoidally loaded at a frequency of 10 Hz and at a constant temperature of $20 \pm 0.5^\circ\text{C}$. The beam fatigue test setup with the LVDT attached can be seen in figure 3.17.



Figure 3.16: GCTS Flexural Beam Setup



Figure 3.17: Beam Fatigue Test Setup with the LVDT Attached

3.8 Indirect Tensile Strength Test

Indirect Tensile (IDT) Strength Test was done according to AASHTO T 283. The sample size of 4 inches (100mm) in diameter and 2.5 ± 1 inches (63.5 ± 2.5 mm) in thickness is maintained. Figures 3.18 and 3.19 display a typical IDT sample with dimensions. The load was applied to the specimen at constant rate of 2 inches/minute (50 mm/minute). A typical IDT test set up with a specimen is shown in figure 3.20. The sample tensile strength is calculated using:

$$S_t = \frac{2P}{\pi tD} \quad (3.7)$$

Where,

S_t = tensile strength, psi

P = maximum load, lbf

t = specimen thickness, inches

D = specimen diameter

The effect of freeze-thaw is further analyzed as the ratio of the original strength that is retained after the freeze-thaw conditioning. The tensile strength ratio is calculated as:

$$\text{Tensile Strength Ratio (TSR)} = \frac{S_2}{S_1} \quad (3.8)$$

Where,

S_1 = average tensile strength of control, kPa

S_2 = average tensile strength of the conditioned, kPa

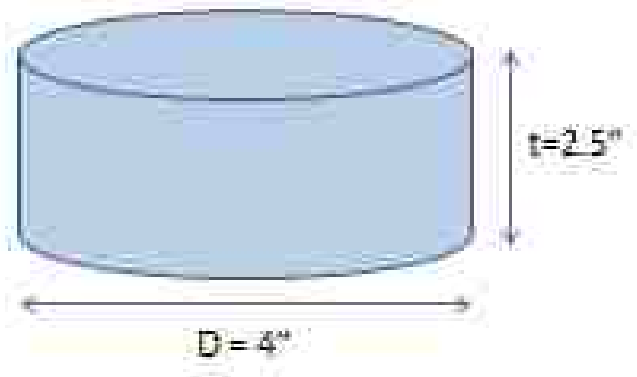


Figure 3.18: IDT Sample with Dimensions



Figure 3.19: IDT Asphalt Concrete Sample



Figure 3.20: IDT Test Setup with a Specimen

3.9 Bending Beam Rheometer Test

The Bending Beam Rheometer (BBR) test is done according to AASHTO T 313. BBR test is used to study the stiffness of binder at low temperatures. Samples are tested at -10°C; Creep stiffness and m-value, which is the slope of the master stiffness curve, is determined. The standard calls for a constant creep load of 980 mN on the asphalt binder beam for 240 seconds and the measured values for stiffness and m-values at 60 seconds are used. The stiffness of the asphalt binder beam is calculated using:

$$S(t) = \frac{PL^3}{4bh^3\delta(t)} \quad (3.9)$$

Where,

$S(t)$ = time-dependent flexural creep stiffness, MPa

P = constant load, N

L = span length, mm

b = width of beam, mm

h = thickness of beam, mm

$\delta(t)$ = deflection of beam, mm

$\delta(t)$ and $S(t)$ indicate that the deflection and stiffness are functions of time.

The time displacement data is extracted for further analysis and stiffness and m-value calculation.

Figure 3.21 and 3.22 show diagram of BBR and the BBR testing apparatus, respectively.

BBR test sample can be seen in figure 3.23.

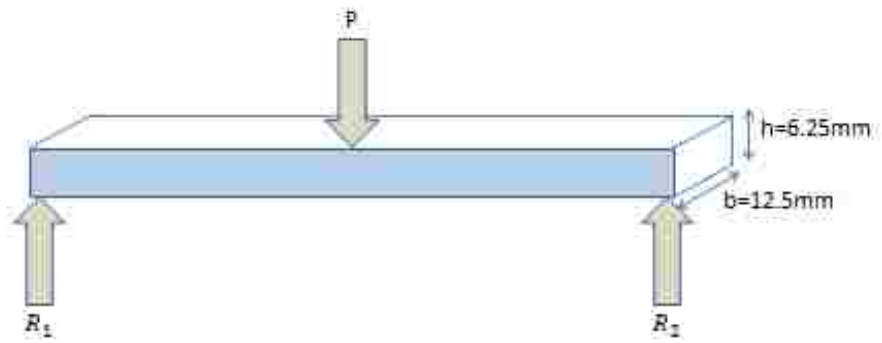


Figure 3.21: BBR Sample with Dimensions



Figure 3.22: BBR Testing Apparatus



Figure 3.23: BBR Test Setup with a Sample

CHAPTER 4

EFFECT OF FREEZE-THAW ON BEAM FATIGUE PARAMETERS

4.1 Introduction

In this section, laboratory test results of flexure beam test are analyzed. The objective of this study is to characterize the evolution of freeze-thaw damage on the decrease of modulus and fatigue life of AC. All samples are conditioned similarly with different freeze-thaw cycles for each set of samples. Table 4.1 presents the test matrix for the four-point bending test. One Hot Mix Asphalt (HMA) mixture was used for this study with a PG 70-22 binder. The material is collected from District 2, New Mexico. The applied strain amplitude is fixed at $400\mu\epsilon$ with the number of freeze-thaw varying from 0 to 20 cycles. The target air voids content in the samples are $5.5 \pm .5\%$.

Table 4.1: Test Matrix for Four-Point Bending Test

HMA mix type	PG binder	Applied Strain	Air Void Content	Freeze-Thaw Cycles
SP-III	70-22	$400\mu\epsilon$	$5.5 \pm .5\%$	0
				5
				10
				15
				20

4.2 Fatigue Test

Asphalt beam flexure tests are conducted using a four-point bending schematic. The tests are performed at $400\mu\epsilon$ amplitude, frequency of 10Hz, and control temperature of $20 \pm .5$ °C. The tests are performed to determine the flexure modulus reduction after each set of freeze-thaw conditioning. Table 4.1 presents the test results for the laboratory flexure test along with the sample ID, freeze-thaw cycle number, air void ratio, initial modulus, and number of cycles to failure.

4.2.1 Results and Discussion on Beam Fatigue Test

In the fatigue test, using the displacement and load history, stiffness was recorded every cycle. In figure 4.1, the initial modulus is plotted against different cycles of freeze-thaw. For each column, 3 different samples are tested and the average modulus obtained is plotted. The average initial modulus of the control is 1,055,093 psi. For 5, 10, 15, and 20 freeze-thaw cycles, the obtained modulus are 999,046 psi, 992,816 psi, 959,765 psi, 878,328 psi, respectively. A trend can be seen, as the number of freeze-thaw cycles increases, the average initial modulus decreases. This finding is in correlation with the fact that freeze-thaw conditioning induces damage into asphalt pavement and the repetitive freeze-thaw promotes increasing damage. The damage causes the initial modulus of the pavement to decrease. Although, the case may be true for the average, different results were found for individual cases. For higher freeze-thaw cycles, it was seen that some samples gave a higher initial modulus than the previous samples. This type of behavior is expected with the conditioning method because freeze-thaw ages the binder. The aging of binder makes the sample stiffer. While this may be true for general

cases, some samples showed a decrease in modulus which suggests the freeze-thaw damage has effect on the adhesion between the binder and aggregate. The result of that is a less stiff material.

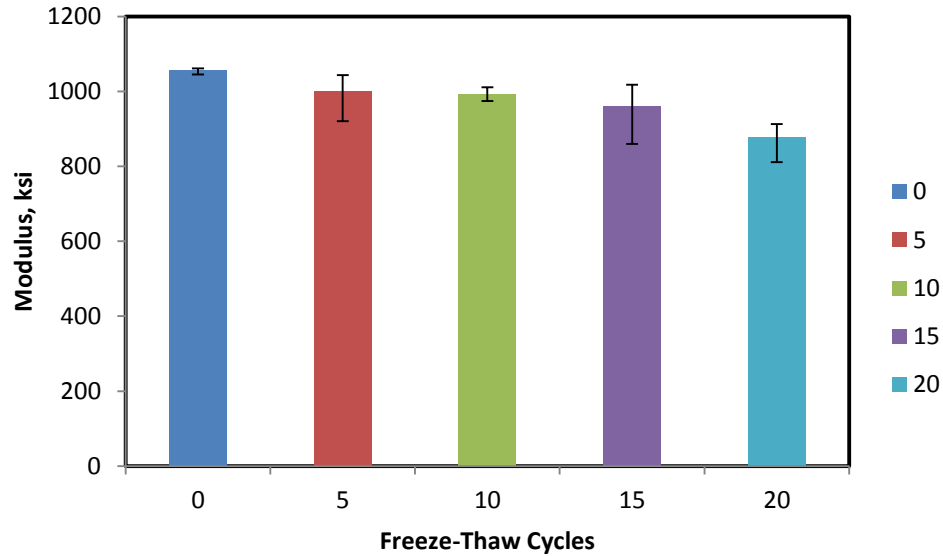


Figure 4.1: Stiffness versus Different Numbers of Freeze-Thaw Cycles Curve

Figure 4.2 compares the fatigue life for different freeze-thaw cycles. It was recorded that the average fatigue life for control (0 freeze-thaw cycles) was 66,601 cycles. For the 5 day freeze-thaw cycle, the average fatigue life decreased to 42,728 cycles. It was seen that the average fatigue life stayed the same, 42,534 cycles to failure. It is worth noting that the most change in fatigue occurred between the 0 and 5 freeze-thaw cycles then the fatigue tends to stabilize. For the 15 freeze-thaw cycles, the fatigue life decreased to 30,868 cycles. 20 freeze-thaw cycles, resulted in higher fatigue life than 15 freeze-thaw cycles. This is due to the behavior of some samples producing higher fatigue lives than of 15 freeze-thaw cycles. It can be seen in table 4.1 that the initial modulus of 20 freeze-thaw cycles are less than 15, yet the produced a greater fatigue life. It is worth noting that

higher initial modulus sometimes does not produce a greater life. As samples age, they become stiffer i.e. more brittle. With the repetitive loading mode, higher initial modulus does not necessarily produce a greater fatigue life, as they will crack sooner.

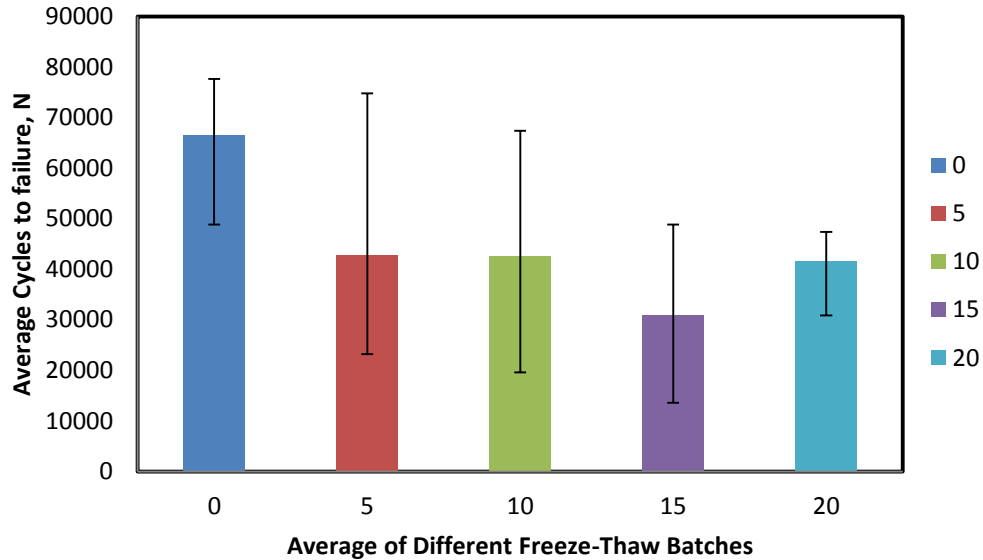


Figure 4.2: Comparison of Number of Cycles to Failure with Different Freeze-Thaw Cycles

Moreover, modulus-number of cycles to failure is plotted for different freeze-thaw cases, shown in figure 4.3. The figure represents a sample from every batch of freeze-thaw. Two things can be noted here, as number of freeze-thaw increases the graph becomes shorter horizontally, i.e. fails quicker. Also, as the number of freeze-thaw cycles increases, the lines on the graph drops lower which indicates a drop in modulus. The result is very acceptable because as predicted, the freeze-thaw conditioning should cause damage to asphalt samples, which should decrease the modulus, as well as have an effect on the fatigue life of asphalt pavement.

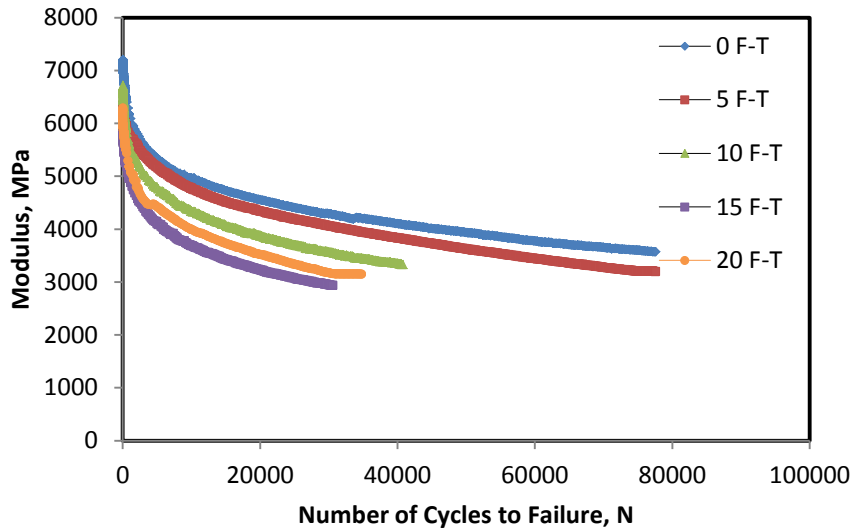


Figure 4.3: Comparison of Modulus Reduction with Different Freeze-Thaw Cycles

Table 4.1: Fatigue Test Results with Different Cycles of Freeze-Thaw

Sample ID	Freeze-Thaw Cycles	Air Voids (%)	Initial Modulus (psi)	Average Initial Modulus (psi)	# of Cycles to Failure	Average Cycles to Failure
D2-2	0	5.8	1,061,641	1,055,093	73,401	66,601
D2-3		5.7	1,058,448		48,801	
D2-4		5.4	1,045,189		77,601	
D2-5	5	5.2	919,974	999,046	74,782	42,728
D2-6		5.4	1,033,798		30,201	
D2-7		5.7	1,043,367		23,201	
D2-8	10	5.9	993,537	992,816	67,401	42,534
D2-9		5.8	1,010,482		19,601	
D2-10		5.6	974,428		40,601	
D2-11	15	5.4	1,017,395	959,765	48,801	30,868
D2-12		5.1	859,870		30,201	
D2-13		5.4	1,002,030		13,601	
D2-14	20	5.2	810,830	878,328	46,773	41,672
D2-15		5.5	911,773		30,841	
D2-16		5.6	912,382		47,401	

Moreover, the results from each test is plotted with their respectively freeze-thaw cycles group. Each plot will represent the initial modulus, modulus reduction and the number of cycles to failure. Figure 4.4 presents sample ID D2-2, D2-3, and D2-4, which were tested under zero freeze-thaw conditioning. The number of cycles is plotted against the modulus. The figure shows the modulus reduction trend. It can be seen that all three samples follow similar failure trend with D2-4 having the greatest fatigue life and D2-3 having the shortest life. Similarly, the results from 5, 10, 15, and 20 freeze-thaw cycles are plotted in figures 4.5, 4.6, 4.7, and 4.8. Comparing all four figures, it can be seen that as the number of freeze-thaw cycles increase, shorter fatigue lives are achieved and the initial modulus also decreases. This is attributed to the phenomena of water being entrapped in the pavement due to moisture and when the temperature reaches freezing, the moisture entrapped in the pavement freezes. When the weather overcomes the freezing temperature, it undergoes thawing, and the repetitive freezing and thawing causes an adhesion loss between binder and aggregate.

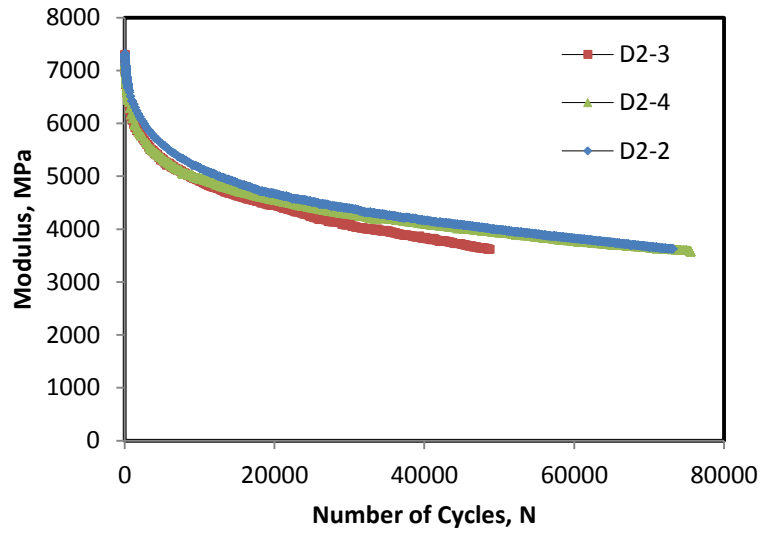


Figure 4.4: Modulus versus Number of Cycles for 0 Freeze-Thaw Cycles

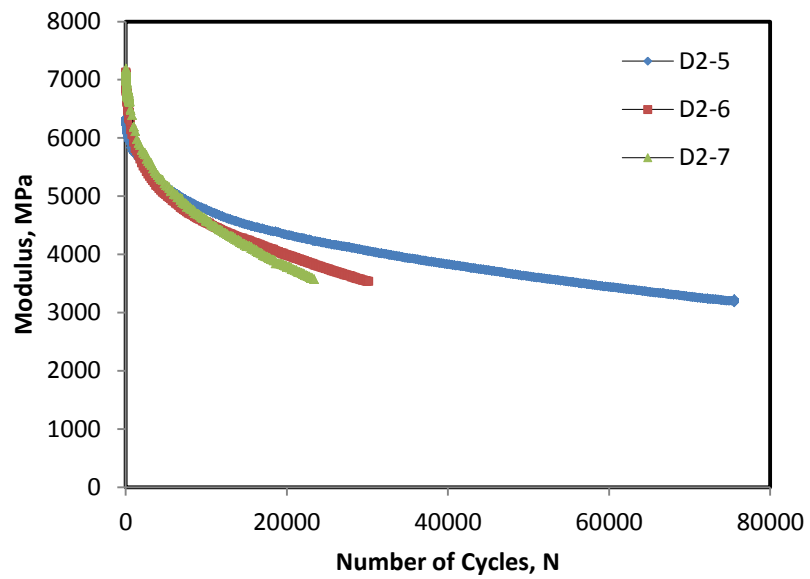


Figure 4.5: Modulus versus Number of Cycles for 5 Freeze-Thaw Cycles

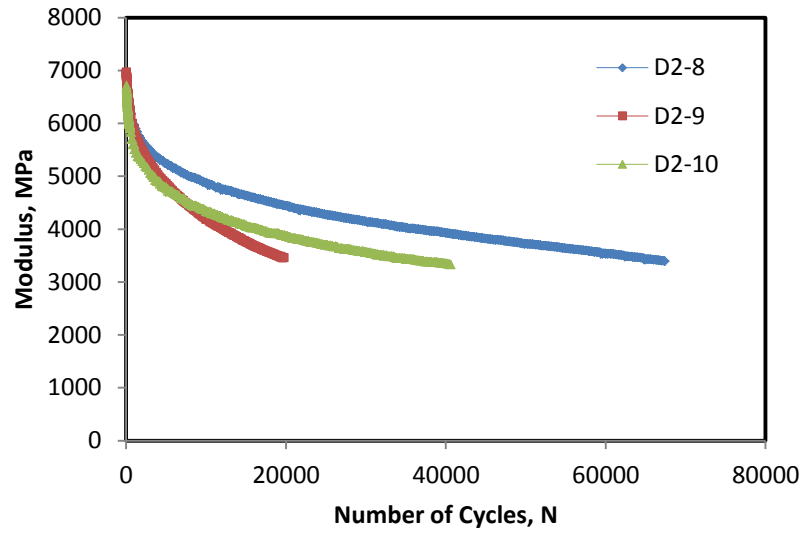


Figure 4.6: Modulus versus Number of Cycles for 10 Freeze-Thaw Cycles

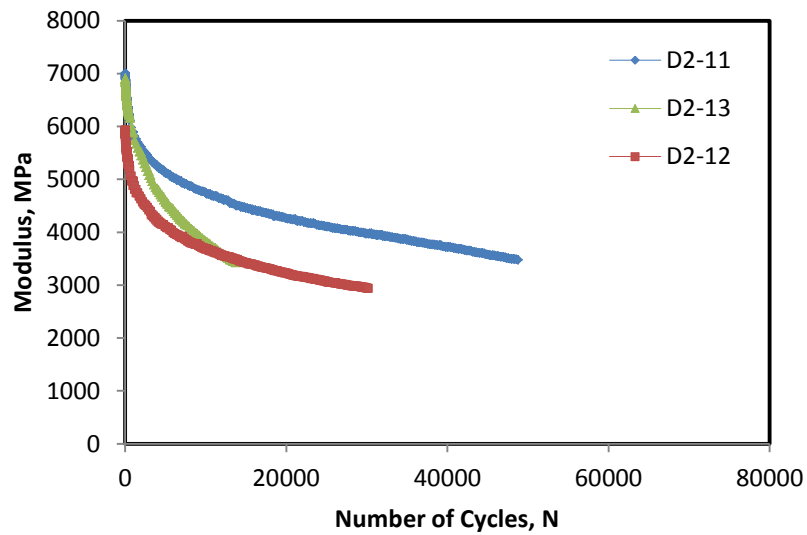


Figure 4.7: Modulus versus Number of Cycles for 15 Freeze-Thaw Cycles

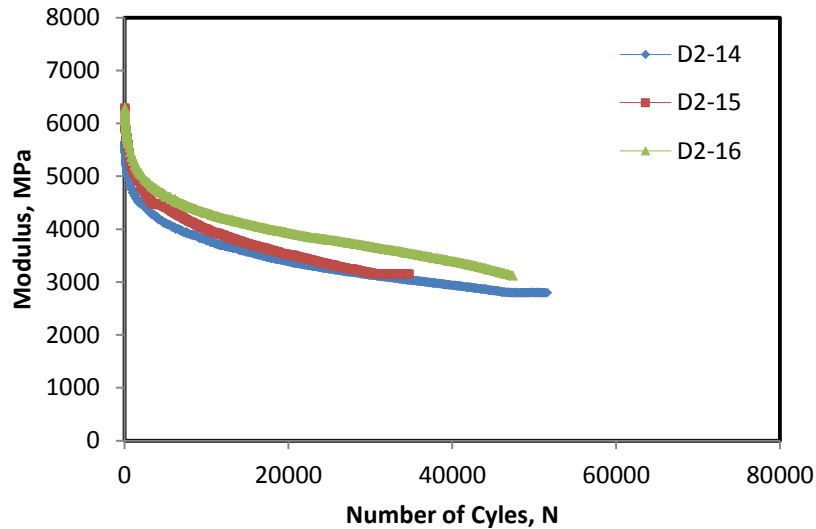


Figure 4.8: Modulus versus Number of Cycles for 20 Freeze-Thaw Cycles

Additionally, modulus ratio is an important parameter in determining the fatigue life. By the AASHTO T 321, the initial modulus is taken at 50 cycles. The initial modulus is used for determining failure, 50% of its initial modulus. Figures 4.9, 4.10, 4.11, 4.12, and 4.13 represent the modulus ratio reduction for 0, 5, 10, 15, 20 freeze-thaw cycles, respectively. The plots are represented with number of cycles to failure versus modulus ratio reduction. Similarly, as the number of freeze-thaw cycles increase, there is a decrease in modulus ratio. The inclusion was freeze-thaw conditioning causes the samples to be less stiff initially as well as lose stiffness during testing. The modulus loss rate determines the failure rate and as the modulus loss rate increases, samples will fail faster.

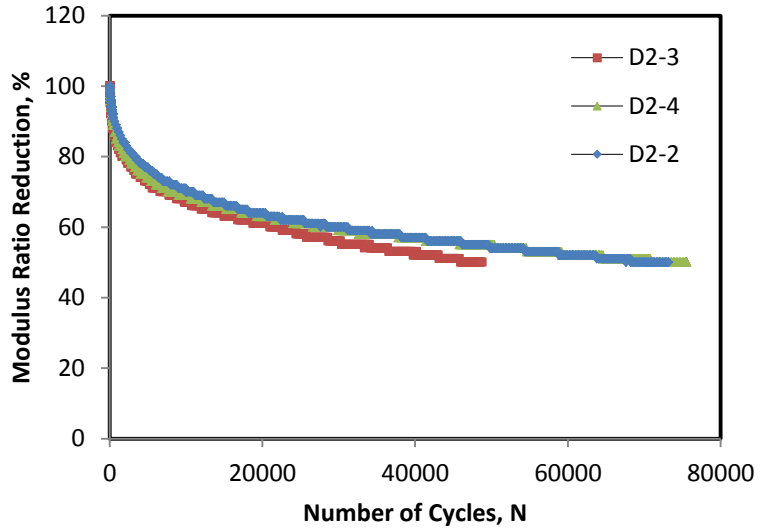


Figure 4.9: Modulus Ratio versus Number of Cycles for 0 Freeze-Thaw Cycles

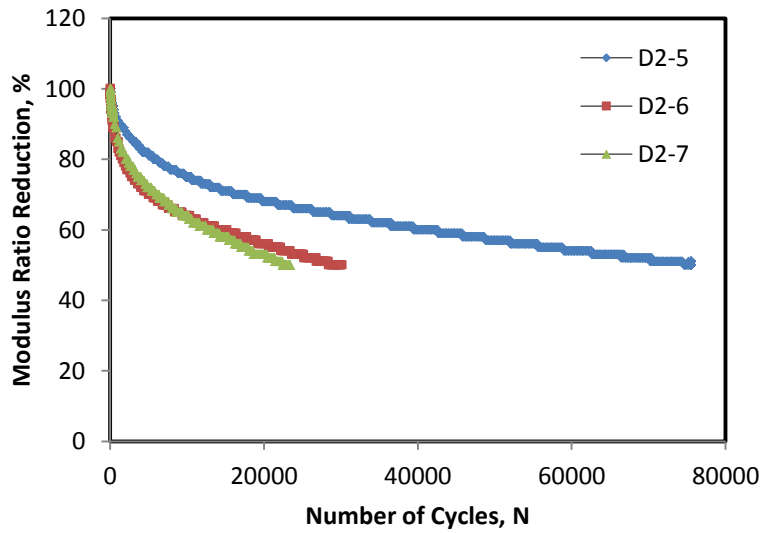


Figure 4.10: Modulus Ratio versus Number of Cycles for 5 Freeze-Thaw Cycles

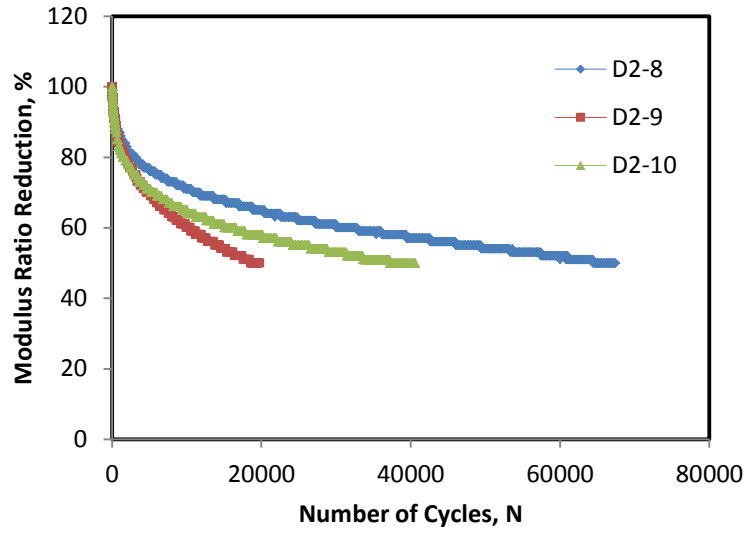


Figure 4.11: Modulus Ratio versus Number of Cycles for 10 Freeze-Thaw Cycles

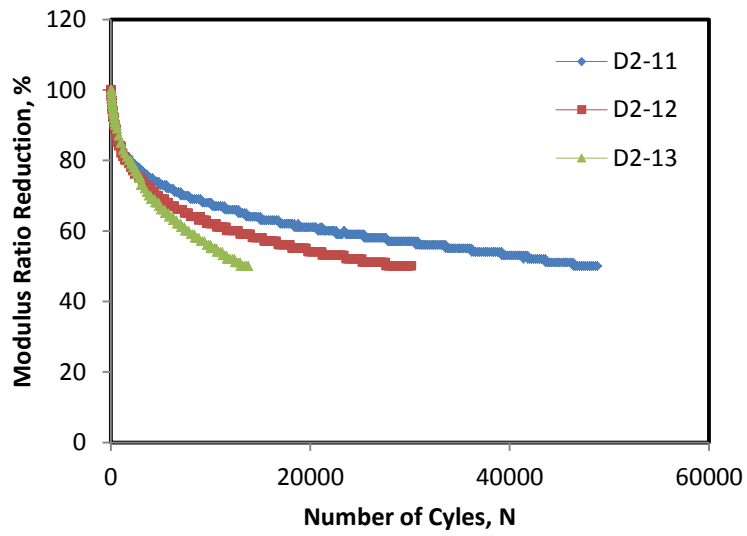


Figure 4.12: Modulus Ratio versus Number of Cycles for 15 Freeze-Thaw Cycles

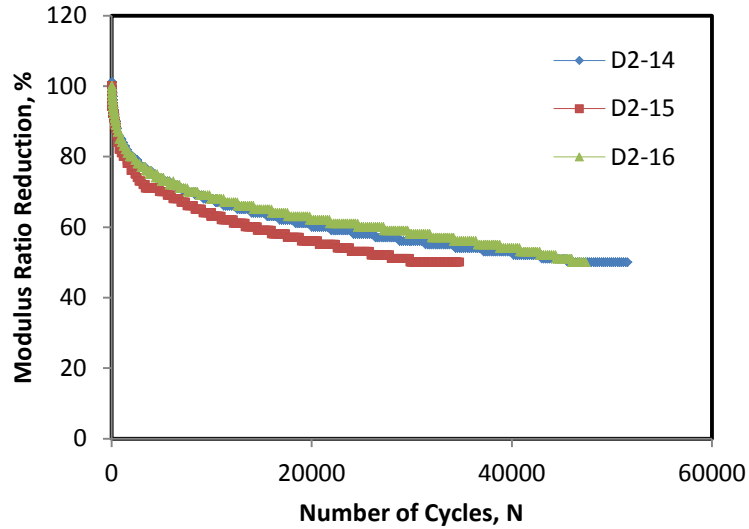


Figure 4.13: Modulus Ratio versus Number of Cycles for 20 Freeze-Thaw Cycles

Furthermore, it is important to correlate the results with an equation. Figure 4.14 shows the freeze-thaw cycles versus average initial modulus. The results for each batch of freeze-thaw is collected and plotted as a point. Each point represents the average of three samples. Using an exponential function to best fit the curve, an equation for the modulus is obtained with a R^2 value of 0.9042. The equation follows as:

$$S = 1000000e^{-0.008f} \quad (4.1)$$

Where,

S = modulus, psi

f = number of freeze-thaw cycles

From this equation, it can be used to predict what the initial modulus for an asphalt sample may be for a particular freeze-thaw cycles. This equation can be used for samples undergoing $400\mu\epsilon$ at $10Hz$ frequency tested at $20^\circ C$.

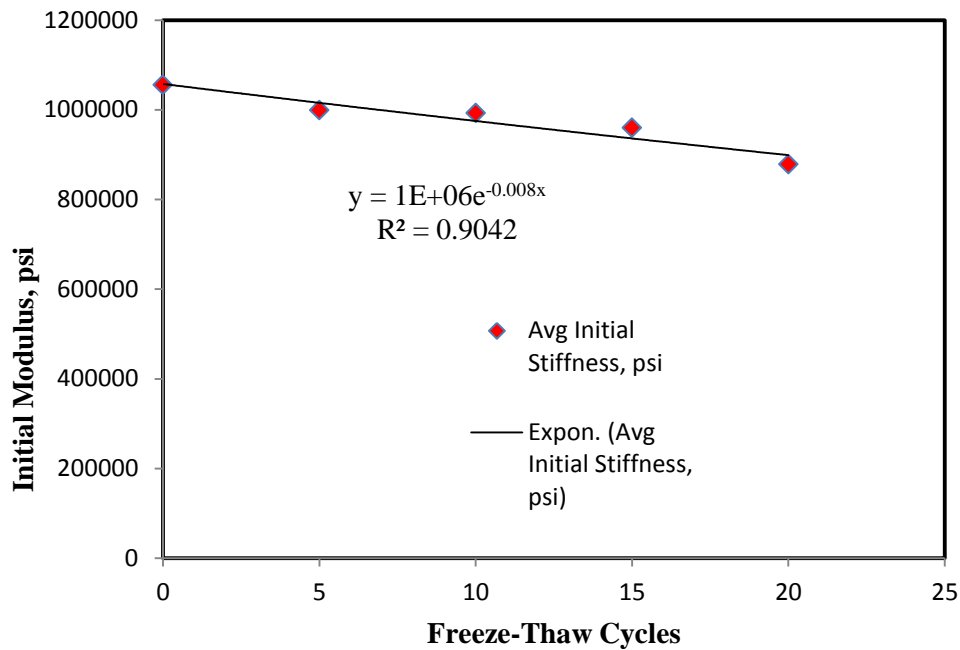


Figure 4.14: Correlation of Initial Modulus with Increasing Number of F-T Cycles

Furthermore, in figure 4.15, the box plot for each class of freeze-thaw shows median, $\frac{1}{4}$ quartile, $\frac{3}{4}$ quartile and variation range of the data. It can be seen that the modulus decreases with increase in freeze-thaw cycle. It can be said that freeze-thaw conditioning is decreasing the modulus of the material and increasing the damage in the sample. Modulus data for each class of freeze-thaw is further analyzed for ANOVA analysis. Data analysis is done in statistical software R. The analysis is done with the assumption that the normality assumption holds true. From ANOVA analysis, for different freeze-thaw cycles, a p-value of 0.06681 is obtained, which is less than 0.1 (90% confidence interval). Therefore, it can be said that there is a statistical difference between the mean of each group. To further analyze which mean is different from the control samples, t-test is used. From t-test, it is seen a statistical difference can be seen after 10 cycles of freeze-thaw.

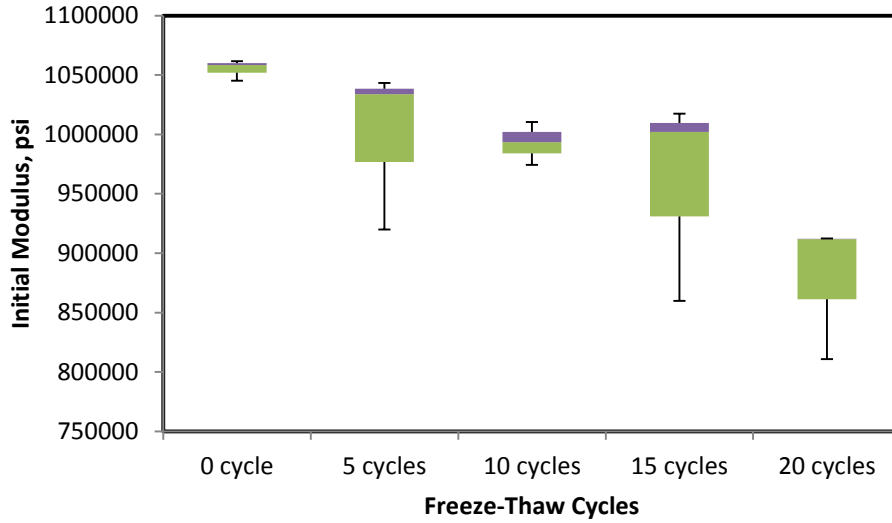


Figure 4.15: Box Plot for Different Cycles of F-T with Their Respective Initial Modulus

Likewise, the number of freeze-thaw cycles to failure is also plotted number of freeze-thaw cycles, shown in figure 4.16. The number of cycles to failure is plotted in log scale on the y axis. Using an exponential function to best fit the data, an equation was obtained with a R^2 value of 0.6327:

$$L = 69270e^{-0.036f} \quad (4.2)$$

Where,

L = number of cycles to failure

f = number of freeze-thaw cycles

It can be seen that the R^2 value less than ideal but a clear trend can be seen. The smaller R^2 is the result of 15 freeze-thaw cycles, where the samples for that particular batch failed sooner than of 20 freeze-thaw cycles. From the above equation, the number of cycles to failure can be predicted with the increasing number of freeze-thaw.

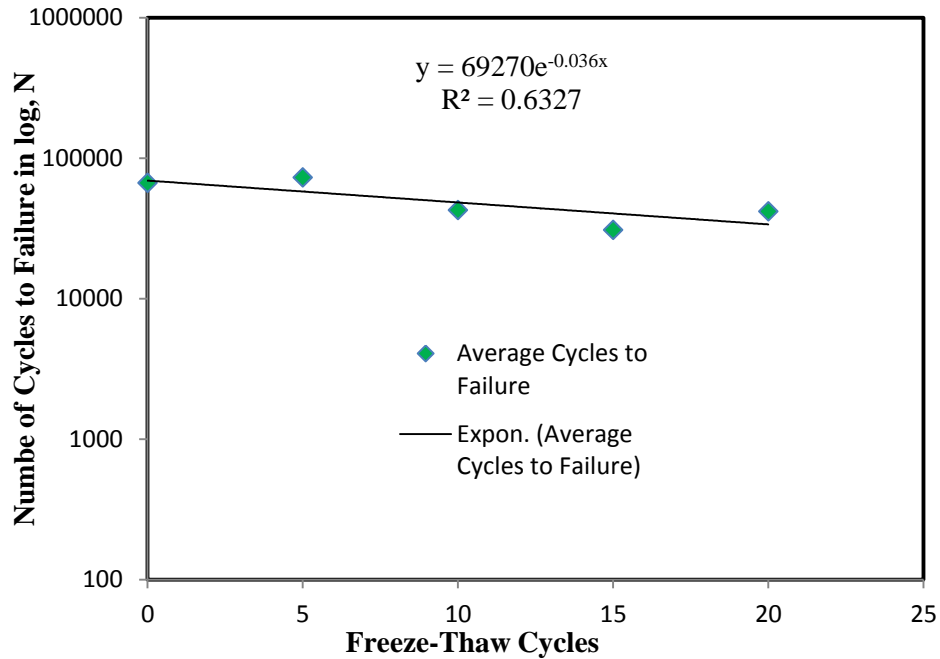


Figure 4.16: Correlation of Number of Cycles to Failure to F-T Cycles

In addition, in figure 4.17, the box plot for each class of freeze-thaw with respect to number of cycles to failure is shown. The figure shows median, $\frac{1}{4}$ quartile, $\frac{3}{4}$ quartile and variation range of the data. It can be seen that there is a decreasing trend in the number of cycles to failure with increasing freeze-thaw. From the box plot, it can be seen a wider range for 5, 10, and 10 freeze-thaw cycles, but the overall trend shows a decrease in fatigue life. From ANOVA analysis, for different freeze-thaw cycles, a p-value of 0.08399 is obtained, which is less than 0.1. The p-value implies there is detectable difference between the mean of each group. Therefore, the mean there is evidence that the mean of each group is different from each other. To further analyze which mean is different from the control sample, t-test is performed. From t-test, it is shown the mean of the 15 days is different than of 0 days.

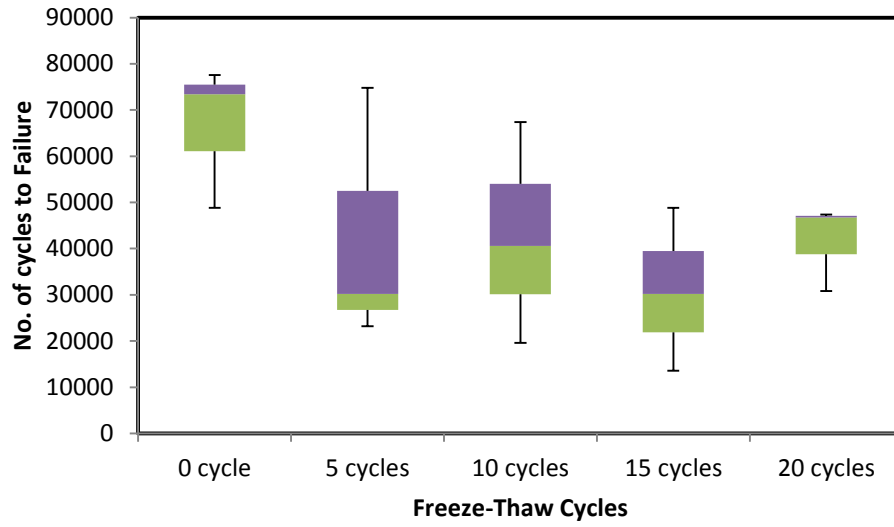


Figure 4.17: Box Plot for No. of Cycles to Failure with Respective F-T Cycles

CHAPTER 5

EFFECTS OF FREEZE-THAW ON INDIRECT TENSILE STRENGTH AND BENDING BEAM RHEOMETER STIFFNESS

5.1 Introduction

In this section, laboratory test results of indirect tensile strength test and bending beam rheometer test are analyzed. The objective of this study is to characterize the evolution of freeze-thaw damage on the decrease of stiffness and strength of AC. All samples are conditioned similarly with different freeze-thaw cycles for each set of samples.

Table 5.1 presents the test matrix for the IDT test. The same mix, collected from the field in District 2 is used for this study. The air voids content is also maintained at $5.5 \pm .5\%$ to maintain uniformity and represent similar gradation. Similarly, the number of freeze-thaw varies from 0 to 20 cycles.

Table 5.2 represents the test matrix for the bending beam rheometer test. The binder grade used for this part of the study is 70-22, the same binder grade used for the HMA. The binder is conditioned under the same freeze-thaw scheme with the cycles varying from 0 to 20.

Table 5.1: Test Matrix for IDT Test

HMA mix type	PG binder	Air Void Content	Freeze-Thaw Cycles
SP-III	70-22	5.5 ± .5%	0
			5
			10
			15
			20

Table 5.2: Test Matrix for Bending Beam Rheometer Test

PG binder	Freeze-Thaw Cycles
70-22	0
	5
	10
	15
	20

5.2 Indirect Tensile Strength Test

Indirect Tensile test was done at room temperature with the load applied at a constant rate of 2 inches/minute (50 mm/minute). The sample sizes are 4 inches in diameter 2.5 inches in height. The IDT test was done to see the effect of freeze-thaw on the indirect tensile strength of asphalt cylinder. The results of the indirect tensile strength and tensile strength ratios are given in table 5.1.

5.2.1 Results and Discussion for IDT Test

Table 5.1 presents the laboratory Indirect Tensile Strength test results for the SP-III 70-22 mixture. The table presents the results for different cycles of freezing and thawing, ranging from 0 freeze-thaw cycles, control, to 20 cycles of freezing and thawing. The IDT strength is given in psi along with its respective sample ID and number of freeze-thaw cycles the sample has undergone. The average IDT strength is presented for the respective batch of freeze-thaw, i.e. 0, 5, 10, 15, 20 cycles. From the average IDT strength, the tensile strength ratio is calculated and presented in table 5.1. For each batch of freeze-thaw, 3 samples were tested and the average is taken to represent the respective freeze-thaw conditioning.

Table 5.3: Laboratory Indirect Tensile Strength and Tensile Strength Ratio

Sample ID	Freeze-thaw cycles	IDT Strength, psi	Median IDT Strength, psi	Tensile Strength Ratio
1	0	162.0	165.7	1
2		172.2		
3		163.0		
4	5	169.2	164.3	0.992
5		163.6		
6		160.2		
7	10	170.4	162.4	0.980
8		162.2		
9		154.5		
10	15	156.4	162.0	0.978
11		157.8		
12		171.9		
13	20	162.0	161.5	0.974
14		158.8		
15		163.6		

For the control, zero freeze-thaw cycles, three samples produced IDT strength of 162, 172.2, and 163 psi, respectively. The average of the three samples were taken, which yielded IDT strength of 165.7 psi. Furthermore, the same procedure was taken for the 5, 10, 15, and 20 freeze-thaw cycles. The average of the 5, 10, 15, 20 freeze-thaw cycles are 164.3, 162.4, 162, 161.5 psi, respectively. Figure 5.1 presents the comparison of the IDT strength with different freeze-thaw cycles. From the table and the graph, it can be seen that after each set of freeze-thaw conditioning, the indirect tensile strength of samples reduced. It can be seen that for the 5 and 10 freeze-thaw, the strength decreased the most,

after which for the 15 and 20 the strength decreases at a lower rate. Figure 5.3 shows the tensile strength ratio with different cycles of freeze-thaw. From control to 5 freeze-thaw cycles, the strength decreased by .845%. For the next batch, the strength decreased by 1.992% from the control to 10 freeze-thaws. For 15 and 20 freeze-thaw cycles, the percent decrease was recorded at 2.233 and 2.535%, respectively. From the reduction of strength with every batch of conditioning, a trend is found, shown in figure 5.2. The best fit curve which produced the highest R^2 was obtained with the exponential function. The exponential function gave a R^2 value of 0.9224, the equation follows as:

$$T = 165.32e^{-.001f} \quad (5.1)$$

Where,

T = Indirect Tensile Strength, psi

f = Number of freeze-thaw cycles

From the equation, the indirect tensile strength can be predicted for any given freeze-thaw cycle. The trend line has a negative slope, which conforms to the literature that when the sample has been induced with conditioning damage, the sample's strength is reduced as well. The equation gives a better understanding of the damage ratio reduction as well as can be used for prediction of damage for longer conditioning.

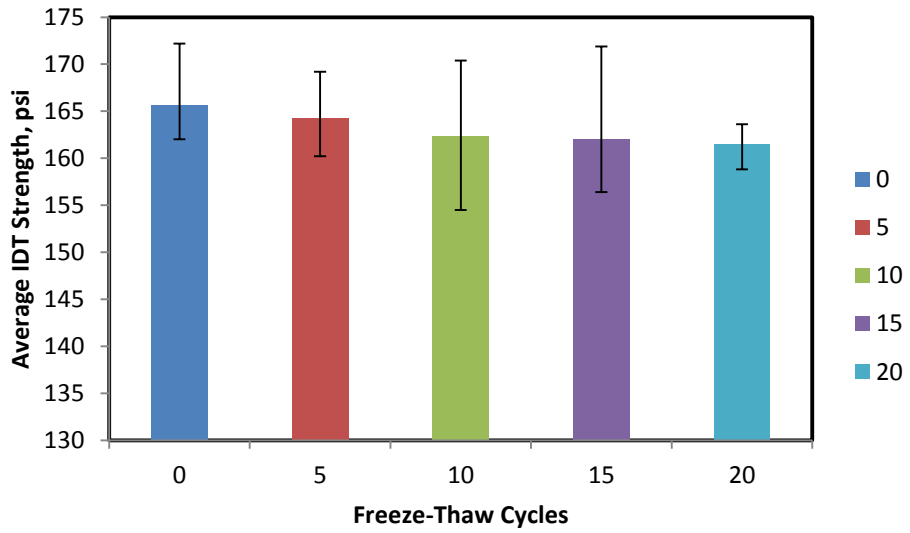


Figure 5.1: Comparison of IDT Strength with different Freeze-Thaw Cycles

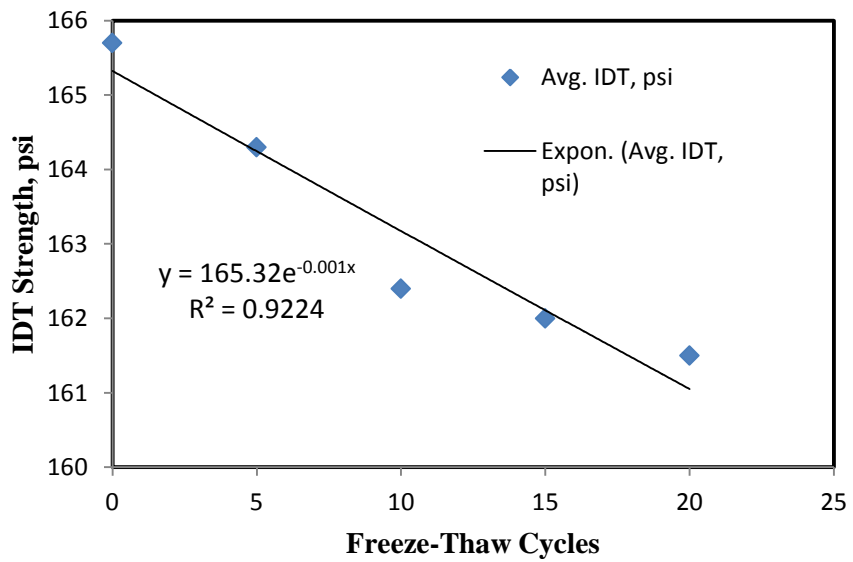


Figure 5.2: Strength Reduction with Different Freeze-Thaw Cycles

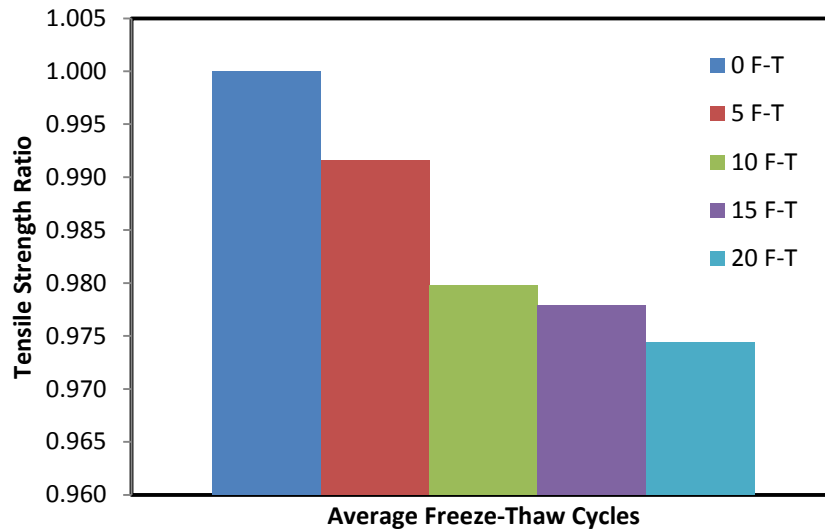


Figure 5.3: Comparison of Tensile Strength Ratio with different Freeze-Thaw Cycles

Figure 5.4 shows the box plot for IDT test for each class of freeze-thaw. The figure shows a steady decrease in strength with increase in freeze-thaw cycle. Therefore, the freeze-thaw cycle is decreasing the strength of the material and increasing the damage in the sample. In addition, 10 cycles of freeze-thaw and 15 cycles of freeze-thaw show a variation, this is due to one sample having a greater strength for their respective groups. Overall, a trend can be seen that there is damage occurring due to freeze-thaw. Although, a decreasing trend can be seen, after ANOVA analysis, no statistical difference is seen between the mean of control and conditioned sample given the confidence interval and sample size. To further understand the damage, more samples should be tested to increase the population size and discard outliers to get a better representative analysis.

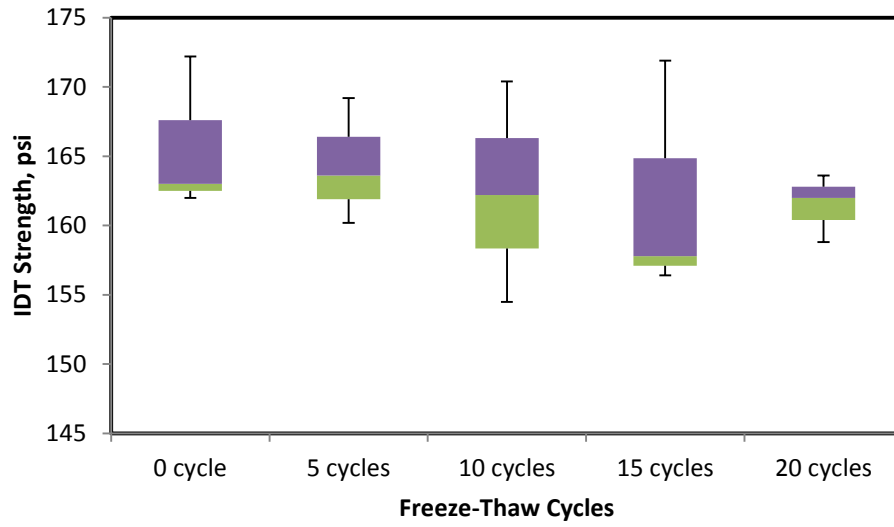


Figure 5.4: Box Plot for IDT Strength with Respective F-T Cycles

5.3 Bending Beam Rheometer Test

Bending Beam Rheometer test is used to study the effect of freeze-thaw on the binder used in the HMA mixture. The results are used to see the stiffness changes at low temperature. All samples are tested at -10°C and the stiffness results are obtained and shown in table 5.4.

5.3.1 Results and Discussion for BBR Test

The current study, attempts to evaluate the effect of freeze-thaw cycles incorporation with the humidity conditioning. To investigate the effect of freeze thaw cycles, the study incorporated flexural creep stiffness of asphalt binder, which has been used to investigate the fatigue stiffness of the material. The study has been done on super pave performance grade (PG) 70-22 binder grade. One control sample without any freeze-thaw conditioning and four samples with 5 cycles, 10 cycles, 15 cycles and 20 cycles of freeze-thaw have been introduced in bending beam Rheometer (BBR) for damage quantification. Three replicate samples for each sample class has been tested in the study. However, additional eight tests repetitions are done for control sample, 5 cycles and 15 cycles of freeze thaw. Repetitions are done due to higher standard deviation for control sample and error in tests for 5 cycle and 15 cycles of freeze-thaw cycles.

Figure 5.5 shows the test data plot obtained for asphalt binder for 20 cycles of freeze-thaw. A creep load of 980 mN remained constant for 240 sec and the deflection is recorded. The maximum deflection found from the test in 5.57 mm. The creep displacement and time data is extracted from the test and modeled to find the stiffness and m-value.

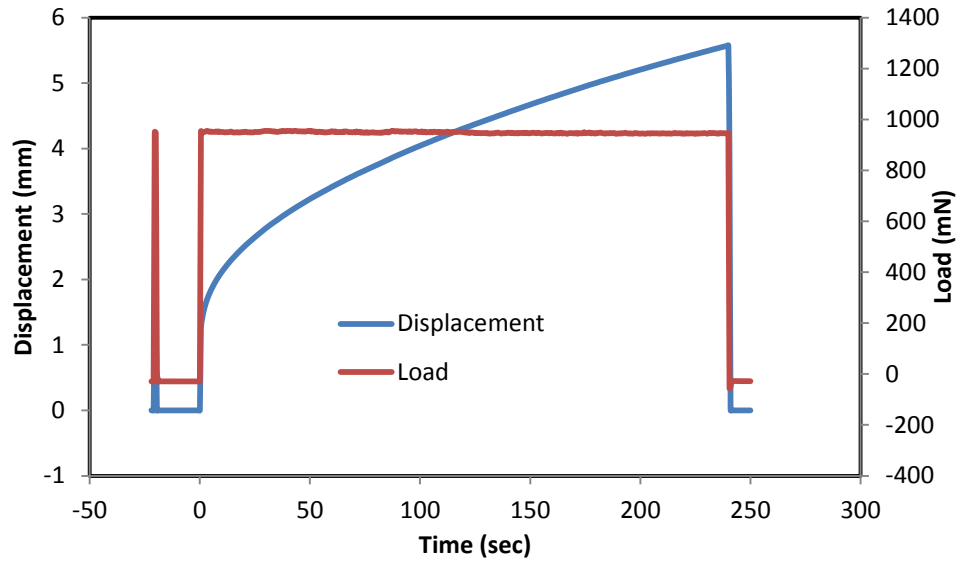


Figure 5.5: Test Data Plot Obtained for Asphalt Binder for 20 cycles of F-T

Figures 5.6, 5.7, 5.8, 5.9, and 5.10 show the load deflection response of zero cycle, 5 cycles, 10 cycles, 15 cycles and 20 cycles of freeze-thaw damaged asphalt binder, respectively. It can be noted that from all the curves maximum displacement found 6.4 mm and minimum of 1.98 mm. The deflection increases for same amount of load as the freeze-thaw cycles increases, which mean freeze thaw cycles damaging the sample by decreasing their stiffness. It can be noted, maximum deflection value is obtained from 15 cycles freeze-thaw damaged sample; however the average maximum displacement leads to 20 cycles freeze-thaw damaged sample.

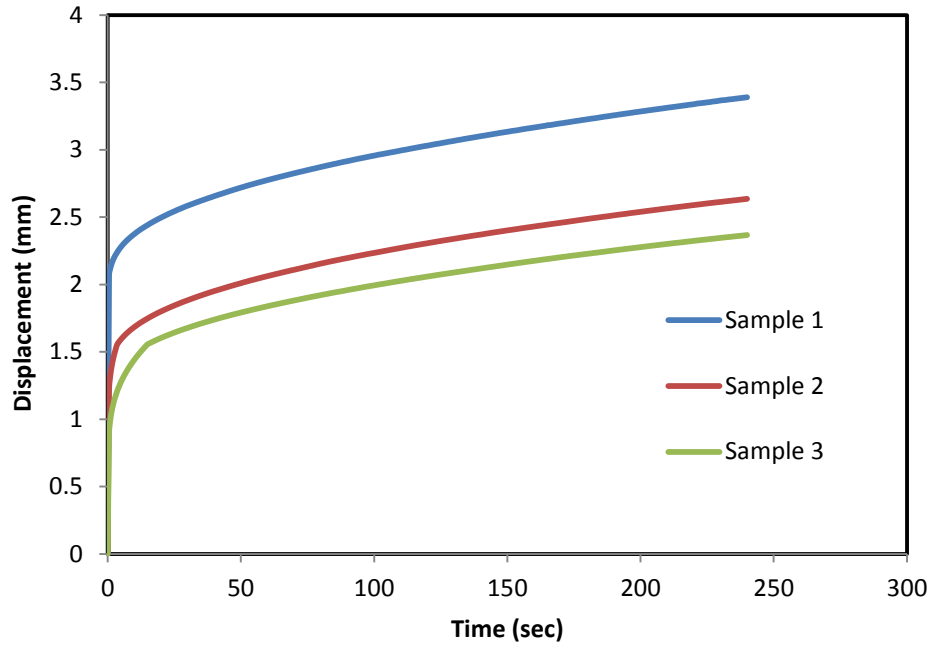


Figure 5.6: Displacement over Time for 0 F-T Cycles

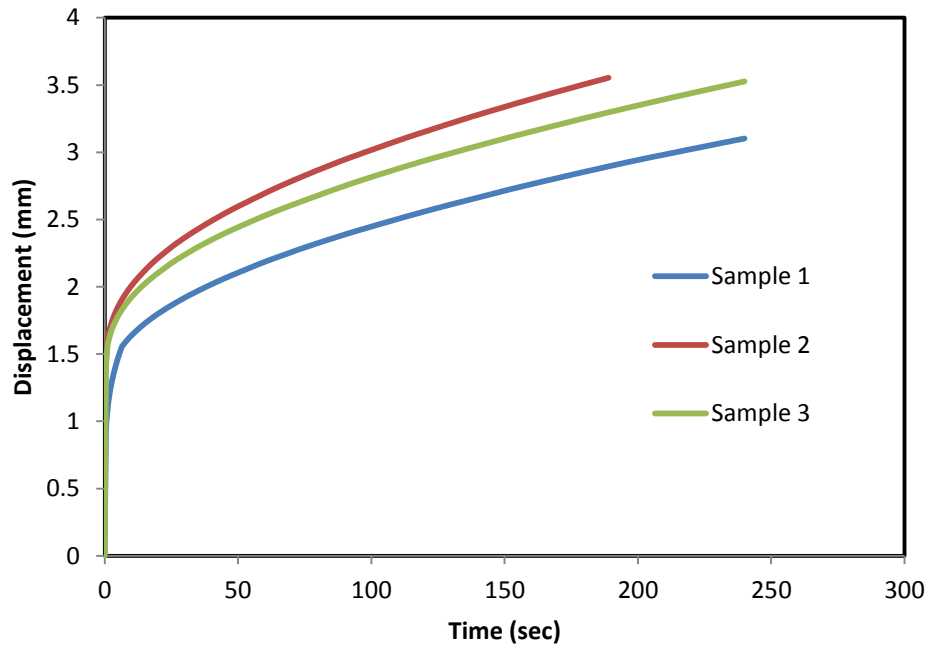


Figure 5.7: Displacement over Time for 5 F-T Cycles

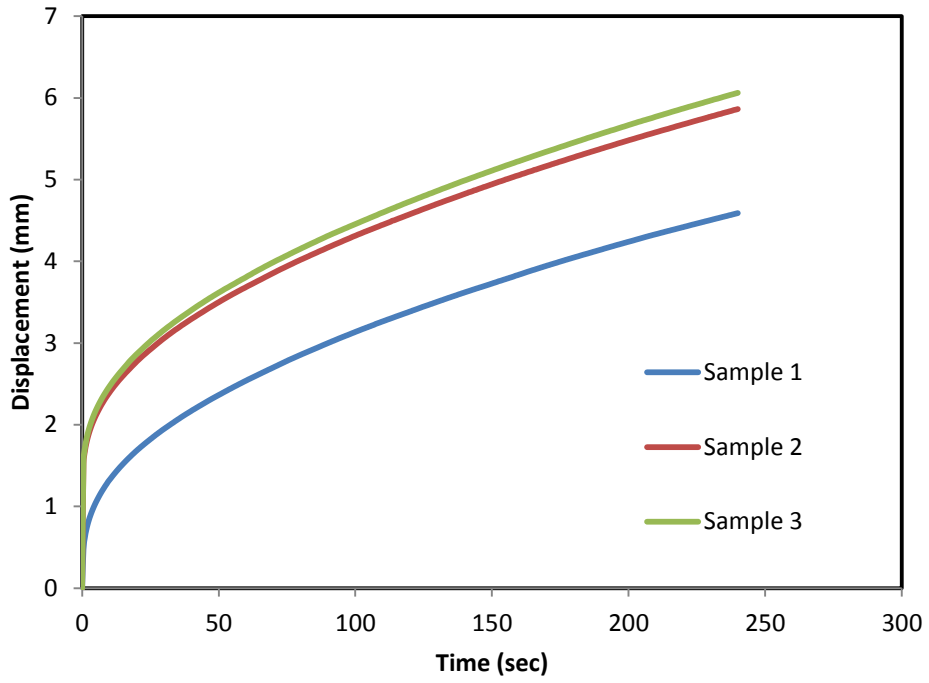


Figure 5.8: Displacement over Time for 10 F-T Cycles

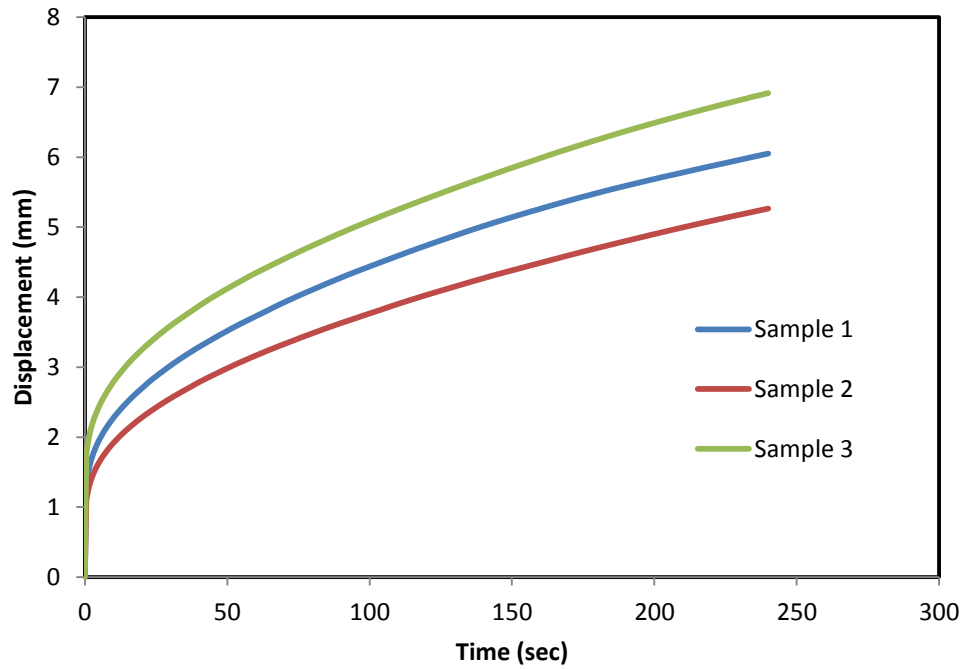


Figure 5.9: Displacement over Time for 15 F-T Cycles

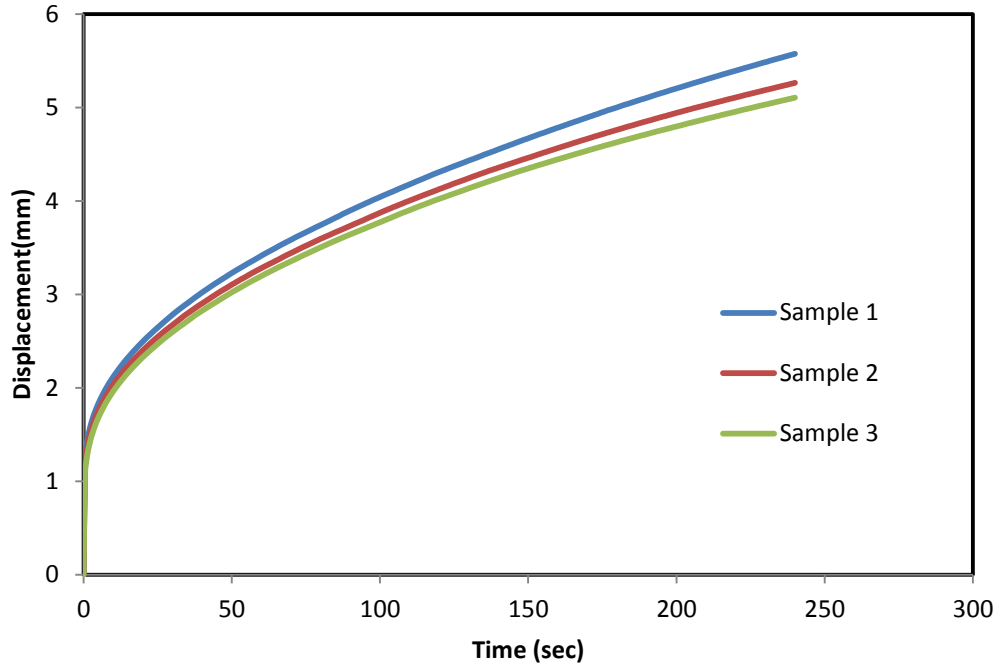


Figure 5.10: Displacement over Time for 20 F-T Cycles

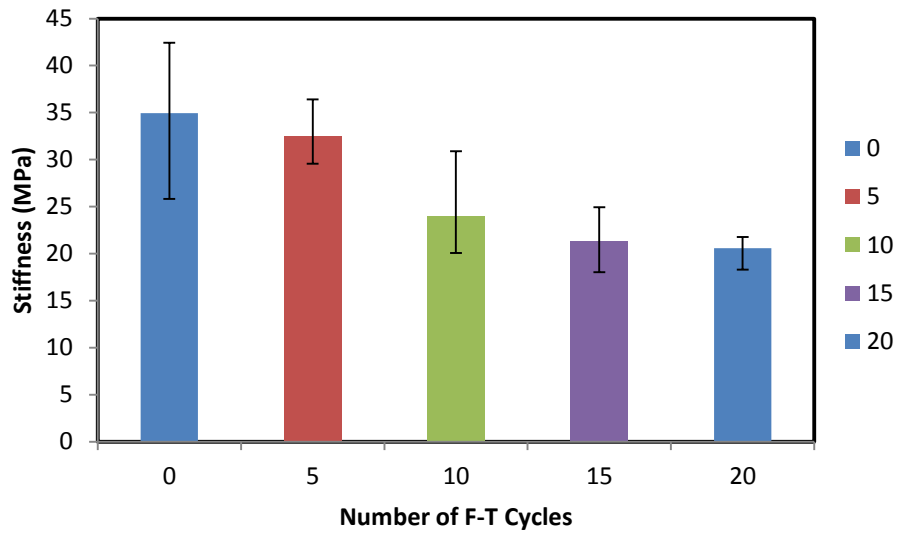


Figure 5.11: Stiffness with Respect to Freeze-Thaw Cycles

The creep test data is introduced into the equation to obtain flexural creep stiffness at -10°C and for m-value of the stiffness vs. logarithmic time is plotted to obtain the slope at any specific time. Figure 5.12 shows the plot of stiffness vs. logarithmic time for m-value or slope calculation for 60 sec. According to stiffness value is calculated for 60 sec for each sample. Three samples for each class of freeze-thaw cycles are analyzed and plotted for statistical analysis, as shown figure 5.13. The box plot for each class show median, $\frac{1}{4}$ quartile, $\frac{3}{4}$ quartile, and variation range of the data. The figure shows the stiffness decreases with increase in freeze-thaw cycle. Therefore, the freeze-thaw cycle is decreasing the stiffness of the material and increasing the damage in the sample. In addition, control sample and 10 cycles freeze-thaw damaged data shows higher variation of data among themselves. Stiffness data for each class freeze-thaw cycle analyzed further for ANOVA analysis. However, the data needs to be analyzed for normality assumption for further analysis. Data analysis is done in statistical software R. For normality assumption, the regression residuals are introduced for Shapiro Wilk test. The analysis shows a p-value of 0.09876 which is greater than 0.05, therefore there is not enough evidence to show that the data does not hold normality assumption. Further, all the data for different freeze-thaw cycles shows a p-value of 0.019822, which is less than 0.05. Therefore, there is enough evidence that the mean of each sample class is different from each other. Doing further statistical analysis, using a t-test with 95% confidence interval, it is shown that a statistical difference is seen after 20 freeze-thaw cycle. It can be said, damage accumulates during the first few cycles of freeze-thaw and after 20 cycles, freeze-thaw has a clear effect on the stiffness of the binder.

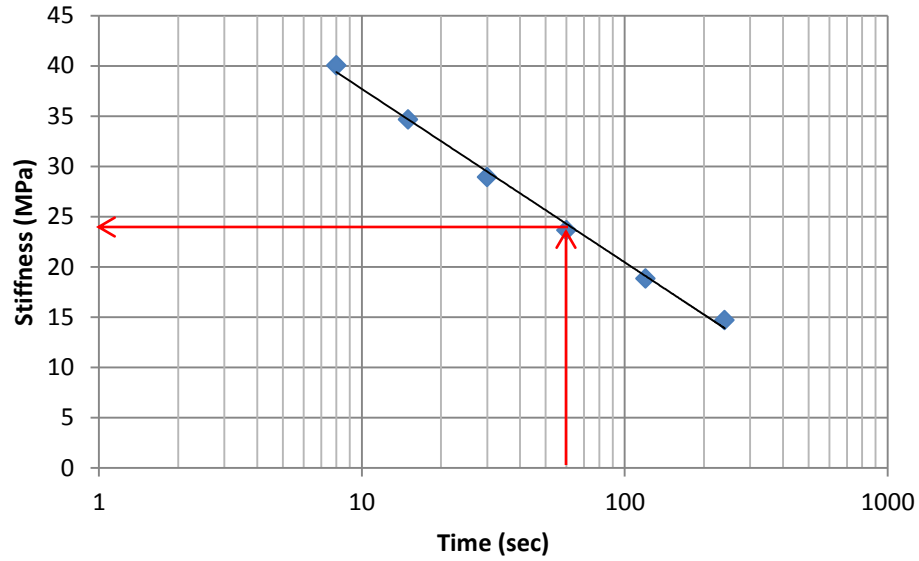


Figure 5.12: plot of stiffness vs. logarithmic time for m-value calculation for 60 sec.

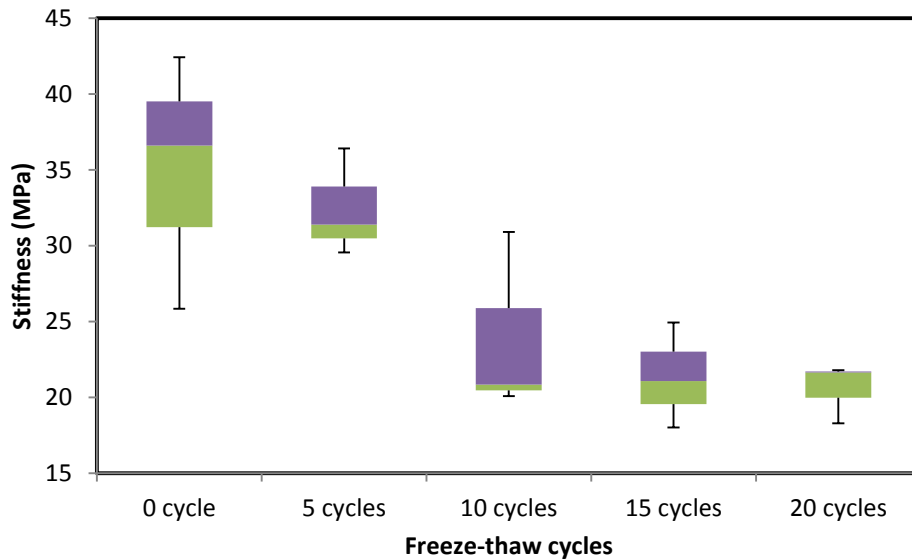


Figure 5.13: Box Plot for different cycles of F-T with their respective Stiffness

Figure 5.14 shows the m-value box plot for each class freeze-thaw cycle. The m-value increases with increase in freeze-thaw cycles. In the BBR stiffness master curve, m-value means the stress relaxation ability. Higher the m-value, higher stress relaxation ability. The figure shows higher stress relaxation ability for higher freeze-thaw cycled asphalt

binder sample. However, m-value median becomes very close to each other after 10 cycles of freeze-thaw, which means stress relaxation becomes almost constant after 10 cycles of freeze-thaw. Therefore, decrease in flexural creep stiffness and increase in stress relaxation ability might be related to increase of viscosity or resistance to flow of asphalt binder with increase in freeze-thaw moisture damage conditioning, which resembles with findings of recent and past literature (M I Hossain, 2013).

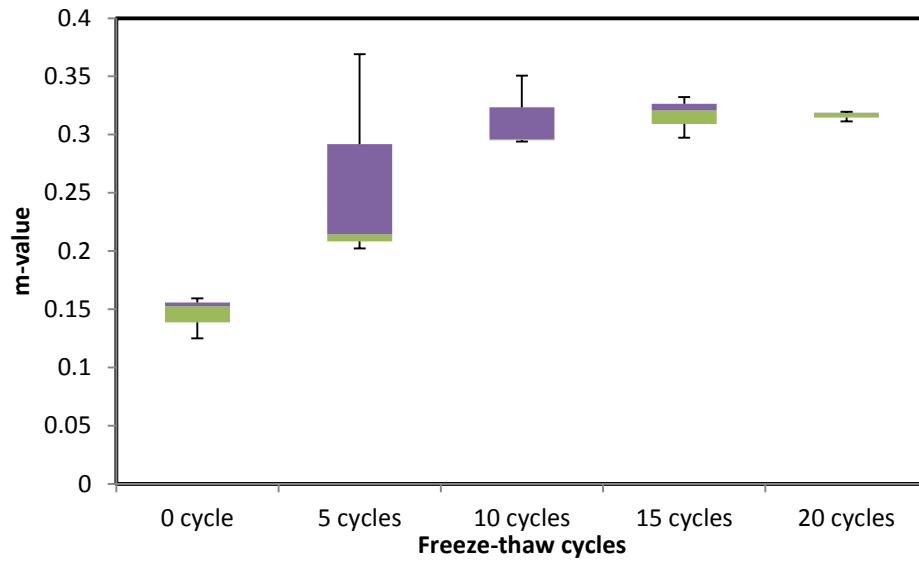


Figure 5.14: m-value Box Plot for Each Class of Freeze-Thaw Cycle

Table 5.4: Stiffness and m-value Test Results for BBR

	Stiffness (MPa)	m-value
Control Sample	25.8273	21.7836
	36.583	21.6341
	42.4156	18.2838
5 Cycles Freeze-thaw	31.381	0.202243
	29.5504	0.369077
	36.4039	0.214423
10 Cycles Freeze-thaw	30.9002	0.350773
	20.8413	0.296275
	20.0666	0.293994
15 Cycles Freeze-thaw	21.0729	0.320713
	24.9219	0.332235
	18.0129	0.297421
20 Cycles Freeze-thaw	21.7836	0.318103
	21.6341	0.319612
	18.2838	0.311261

CHAPTER 6

CONCLUSIONS AND RECOMMENDATIONS

6.1 Conclusions

Several conclusions have been found following the completion of the study on the fatigue test, indirect tensile strength test, and bending beam rheometer test. The conclusions are as follows:

6.1.1 Fatigue Test Conclusion

- It is shown that freeze-thaw conditioning initiates damage in pavement due to moisture entering pavement and causing the bond between binder and aggregate to weaken. In this study, by incorporating four-point bending test, it is seen that freeze-thaw conditioning has a negative effect on the asphalt pavement samples, i.e. reducing the stiffness of the samples.
- Freeze-thaw conditioning also shows an effect on the fatigue of the asphalt samples. Samples which were introduced to freeze-thaw conditioning have a lesser fatigue life. Samples met the failure criteria sooner when subjected to freeze-thaw, than of the control. Fatigue life of the pavement decreased by 35.8%, 36.1%, 53.6%, 37.4% for 5, 10, 15, and 20 freeze-thaw cycles.
- freeze-thaw conditioning decreases the stiffness by 5.3%, 5.9%, 9.0%, 16.8% for 5, 10, 15, and 20 freeze-thaw cycles.
- A regression model for the initial stiffness with respect to number of freeze-thaw cycles is generated. From this model, the initial stiffness of the asphalt samples

can be predicted for any number of freeze-thaw cycles when tested at $400\mu\epsilon$ at $10Hz$ frequency tested at $20^{\circ}C$. The equation is as follows:

$$S = 1000000e^{-0.008f}$$

Where,

S = stiffness, psi

f = number of freeze-thaw cycles

- Additionally, a regression model for the fatigue life of asphalt samples in term of freeze-thaw cycles is also developed. This model can predict the fatigue life of asphalt pavement samples when tested at $400\mu\epsilon$ at $10Hz$ frequency and $20^{\circ}C$. The model follows as:

$$L = 69270e^{-0.036f}$$

Where,

L = number of cycles to failure

f = number of freeze-thaw cycles

6.1.2 IDT Test Conclusion

- Statistically, freeze-thaw conditioning does not have a clear effect on the tensile strength of asphalt pavement. A decreasing tend can be seen in the strength, but there is not enough evidence to conclude that freeze-thaw reduces the strength given the number of samples tested and the confidence interval.

6.1.3 BBR Test Conclusion

- Freeze-thaw cycles for inducing moisture damage in asphalt binder decrease the thermal stiffness or thermal stress capacity of asphalt binder.
- Increase in freeze-thaw cycle increases m-value obtained from stiffness master curve. The increase in m-value means increase in stress relaxation ability of asphalt binder, which might be related to increase of viscosity of asphalt binder for moisture damage.
- Flexural creep stiffness of asphalt binder decreases with increase in freeze-thaw cycles. Stiffness decreased by 7.1%, 31.5%, 38.9%, and 41.1% for 5, 10, 15, and 20 freeze-thaw cycles

6.2 Recommendations for Future Work

- Currently, cylindrical dynamic modulus test is used to determine dynamic modulus of asphalt concrete. These values are used in MEPDG for determining rutting and fatigue. Therefore, fatigue test on cylindrical sample may be thought-provoking and can be done in the future with similar conditioning methods.
- To further investigate into this study, it is recommended to correlate values attained in the lab to field values.
- Furthermore, additional freeze-thaw cycles can be incorporated to determine and verify the behavior of the asphalt concrete and binder.
- Moreover, more extreme cases of weather pattern can be looked at. In Alaska, weather reaches freezing temperatures as cold as -40°C , it may be of interest to investigate lower temperature and evaluate damage.

REFERNCES

- AASHTO T 168-07. Standard Test Method for Sampling Bituminous Paving Mixtures, *American Association of State Highway and Transportation Officials (AASHTO)*, Washington D.C., (2007).
- AASHTO T 269-07. “Standard Method of Test for Percent Air Voids in Compacted Dense and Open Asphalt Mixtures.” *American Association of State Highway and Transportation Officials (AASHTO)*, Washington D.C., (2007).
- AASHTO T321-07. “Standard Test Method for Determining the Fatigue Life of Compacted Hot-Mix Asphalt (HMA) Subjected to Repeated Flexural Bending.” *American Association of State Highway and Transportation Officials (AASHTO)*, Washington D.C., (2007).
- AASHTO T322-07. “Standard Method of Test for Determining the Creep Compliance and Strength of Hot-Mix Asphalt (HMA) Using the Indirect Tensile Test Device.” *American Association of State Highway and Transportation Officials (AASHTO)*, Washington D.C., (2007).
- AASHTO T283-07. “Standard Method of Test for Resistance of Compacted Asphalt Mixtures to Moisture-Induced Damage.” *American Association of State Highway and Transportation Officials (AASHTO)*, Washington D.C., (2007).
- AASHTO T313-08. “Standard Method of Test for Determining the Flexural Creep Stiffness of Asphalt Binder Using the Bending Beam Rheometer (BBR).”

American Association of State Highway and Transportation Officials (AASHTO), Washington D.C., (2008).

AASHTO T312-04. "Standard Method of Test for Preparing and Determining the Density of Hot-Mix Asphalt (HMA) Specimens by Means of the Superpave Gyrotory Compactor." *American Association of State Highway and Transportation Officials (AASHTO), Washington D.C., (2004).*

ASTM C666.C666M. "Standard Test Method for Resistance of Concrete to Rapid Freezing and Thawing." *American Society for Testing and Materials (ASTM), West Conshohocken, PA., (2008).*

ASTM C1645/C1645M. "Standard Test Method for Freeze-thaw and De-icing Salt Durability of Solid Concrete Interlocking Paving Units" *American Society for Testing and Materials (ASTM), West Conshohocken, PA., (2012).*

ASTM D6857/D6857M-11. "Standard Test Method for Maximum Specific Gravity and Density of Bituminous Paving Mixtures Using Automatic Vacuum Sealing Method." *American Society for Testing and Materials (ASTM), West Conshohocken, PA., (2011).*

Carpenter, S. H., Ghuzlan, K. A., and Shen, S. (2003). "Fatigue Endurance Limit for Highway and Airport Pavement." *Transportation Research Record*, No. 1832, pp. 131-138.

Dave, E. V., Braham, A. F., Buttlar, W. G., and Paulino, G. H., (2011). "Development of a Flattened Indirect Tension Test for Asphalt Concrete." *Journal of Testing and Evaluation*, Volume 29, issue 3.

- Schmidt, R. J., (1974). "Effect of Temperature, Freeze-Thaw, and Various Moisture Conditions on the Resilient Modulus of Asphalt-Treated Mixes." *Journal of Transportation Research Record*, Volume 480, issue 515, pp. 27-39.
- Goh, S. and You, Z., (2012). "Evaluation of Hot-Mix Asphalt Distress under Rapid Freeze-Thaw Cycles Using Image Processing Technique." *Journal of American Society of Civil Engineers*, volume 12, pp. 3305-3315.
- Timm, D. H., Robbins, M. M., Willis, J. R., Tran, N., and Taylor, A. J., (2012). "Evaluation of Mixture Performance and Structural Capacity of Pavements Capacity of Pavements Utilizing Shell Thiopave." *National Center for Asphalt Technology, Construction, Laboratory Evaluation and Full-Scale Testing of Thiopave® Test Sections – Final Report*.
- Chen, X., and Huang, B., (2008). "Evaluation of Moisture Damage in Hot Mix Asphalt Using Simple Performance and Superpave Indirect Tensile Tests." *Journal of Elsevier, Construction and Building Materials*, No. 22, 1950–1962.
- Mei, Y., Liang, N., Cao, and Y., Li, Z., (2010). "Fatigue Life Prediction of Asphalt Pavement Based on Cumulative Damage." *Preceding's of the Conference, International Conference on Mechanic Automation and Control Engineering*, Wuhan, pp. 2876-2882.
- Coni, M., (2008). "FE Evaluation of 4-point Bending Test for Fatigue Cracking Assessment." *Pavement Cracking: Mechanisms, Modeling, Detection, Testing and Case Histories*, pp. 271-281.
- Feng, D., Yi, J., Wang, L., and Wang, D., (2009). "Impact of Gradation Types on Freeze-Thaw Performance of Asphalt Mixtures in Seasonal Frozen Region." *Journal of*

American Society of Civil Engineers, Critical Issues in Transportation Systems Planning, Development, and Management, pp. 2336-2342.

Feng, D., Yi, J., Wang, L., and Wang, D., (2010). "Impact of salt and freeze–thaw cycles on performance of asphalt mixtures in coastal frozen region of China." *Journal of Elsevier, Cold Regions Science and Technology*, No 62, pp. 34-41.

Lu, Q., and Harvey, J. T., (2008). "Inclusion of Moisture Effect in Fatigue Test for Asphalt Pavements." *Transportation and Development Innovative Best Practices 2008: Proceedings of the First International Symposium, China*, pp. 511-517.

Liu, Q., Wu, S., and Schlangen, E. (2013). "Induction heating of asphalt mastic for crack control". *Journal of Elsevier, Cold Regions Science and Technology*, No. 41, pp. 345-351.

Özgan, E., and Serin, S., (2012). "Investigation of certain engineering characteristics of asphalt concrete exposed to freeze–thaw cycles." *Journal of Elsevier, Cold Regions Science and Technology*.

Shu, X., Huang, B., and Vukosavljevic, D., (2008). "Laboratory evaluation of fatigue characteristics of recycled asphalt mixture." *Journal of Elsevier, Construction and Building Materials*, No. 22, pp. 1323–1330.

Shu, X., Huang, B., Shrum, E. D., and Jia, X., (2012). "Laboratory evaluation of moisture susceptibility of foamed warm mix asphalt containing high percentages of RAP." *Journal of Elsevier, Construction and Building Materials*, No. 35, pp. 125-130.

- Bolzan, P.E., (1989). "Moisture Susceptibility Behavior of Asphalt Concrete and Emulsified Asphalt Mixtures Using the Freeze-Thaw Padestal Test." *Transportation Research Record*, volume no. 1228, pp. 9-16.
- Christensen, D.W., and Bonaquist, R. F., (2004) "Evaluation of Indirect Tensile Test (IDT) Procedures for Low-Temperature Performance of Hot Mix Asphalt". *National Cooperative Highway Research Program, Report 530, Washington D.C.*
- Pan, P., Sun, C., Tang, N., Chen, M., and Wu, S., (2013). "Study on Volume Performance of Conductive Asphalt Concrete Based on Freeze-thaw Cycle." *Applied Mechanics and Materials*, Vols. 303-306, pp. 2501-2504.
- Huang, S., Robertson, R. E., Branthaver, J. F., Petersen, C. J., (2005). "Impact of Lime Modification of Asphalt and Freeze-Thaw Cycling on the Asphalt-Aggregate Interaction and Moisture Resistance to Moisture Damage." *Journal of Materials in Civil Engineering*, Vol. 17, No. 6, pp. 711-718.
- Poulikakos, L. D., and Partl, M. N., (2009). "Evaluation of Moisture Susceptibility of Porous Asphalt Concrete Using Water Submersion Fatigue Tests." *Journal of Elsevier, Construction and Building Materials*. No. 23, pp. 3475-3484.